



**QUEEN'S  
UNIVERSITY  
BELFAST**

## **Klebsiella pneumoniae survives within macrophages by avoiding delivery to lysosomes**

Cano, V., March, C., Insua, J. L., Aguiló, N., Llobet, E., Moranta, D., Regueiro, V., Brennan, G. P., Millán-Lou, M. I., Martin, C., Garmendia, J., & Bengoechea, J. A. (2015). *Klebsiella pneumoniae* survives within macrophages by avoiding delivery to lysosomes. *Cellular Microbiology*, 17(11), 1537-1560.  
<https://doi.org/10.1111/cmi.12466>

**Published in:**  
Cellular Microbiology

**Document Version:**  
Peer reviewed version

**Queen's University Belfast - Research Portal:**  
[Link to publication record in Queen's University Belfast Research Portal](#)

### **Publisher rights**

©2015 John Wiley & Sons, Inc.

This is the peer reviewed version of the following article: Cano, V., March, C., Insua, J. L., Aguiló, N., Llobet, E., Moranta, D., Regueiro, V., Brennan, G. P., Millán-Lou, M. I., Martin, C., Garmendia, J., Bengoechea, J. A. (2015). *Klebsiella pneumoniae* survives within macrophages by avoiding delivery to lysosomes. *Cellular Microbiology*, VOL: PAGE NO's. which has been published in final form at <http://onlinelibrary.wiley.com/doi/10.1111/cmi.12466/abstract>. This article may be used for non-commercial purposes in accordance with Wiley Terms and Conditions for Self-Archiving.

### **General rights**

Copyright for the publications made accessible via the Queen's University Belfast Research Portal is retained by the author(s) and / or other copyright owners and it is a condition of accessing these publications that users recognise and abide by the legal requirements associated with these rights.

### **Take down policy**

The Research Portal is Queen's institutional repository that provides access to Queen's research output. Every effort has been made to ensure that content in the Research Portal does not infringe any person's rights, or applicable UK laws. If you discover content in the Research Portal that you believe breaches copyright or violates any law, please contact [openaccess@qub.ac.uk](mailto:openaccess@qub.ac.uk).

### **Open Access**

This research has been made openly available by Queen's academics and its Open Research team. We would love to hear how access to this research benefits you. – Share your feedback with us: <http://go.qub.ac.uk/oa-feedback>

1 ***Klebsiella pneumoniae* survives within macrophages by avoiding delivery to lysosomes.**

2 Victoria Cano<sup>1,2†</sup>, Catalina March<sup>1,2†</sup>, Jose Luis Insua<sup>3†</sup>, Nacho Aguiló<sup>2,5</sup>, Enrique Llobet<sup>1,2,4</sup>, David  
3 Moranta<sup>1,2,4</sup>, Verónica Regueiro<sup>1,2,4</sup>, Gerry P Brenan<sup>6</sup>, Maria Isabel Millán-Lou<sup>2,5</sup>, Carlos Martín<sup>2,5</sup>,  
4 Junkal Garmendia<sup>2,7</sup>, José A. Bengoechea<sup>3,8</sup>.

5 Laboratory Infection and Immunity, Fundació d'Investigació Sanitària de les Illes Balears (FISIB),  
6 Bunyola, Spain<sup>1</sup>; Centro de Investigación Biomédica en Red Enfermedades Respiratorias  
7 (CIBERES), Bunyola, Spain<sup>2</sup>; Centre for Infection and Immunity, Queen's University Belfast,  
8 Belfast, United Kingdom<sup>3</sup>; Institut d'Investigació Sanitària de Palma (IdISPa), Palma, Spain<sup>4</sup>; Grupo  
9 de Genética de Micobacterias, Dpto. Microbiología, Medicina Preventiva y Salud Pública,  
10 Universidad de Zaragoza, Zaragoza, Spain<sup>5</sup>; School of Biological Sciences, Queen's University  
11 Belfast, Belfast, United Kingdom<sup>6</sup>; Instituto de Agrobiotecnología, CSIC-Universidad Pública de  
12 Navarra-Gobierno de Navarra, Mutilva, Spain<sup>7</sup>; Consejo Superior de Investigaciones Científicas  
13 (CSIC), Madrid, Spain<sup>8</sup>

14 † These authors contributed equally to this work.

15

16 \*Corresponding author:

17 Prof. José A. Bengoechea

18 Centre for Infection and Immunity,

19 Queen's University Belfast

20 Health Sciences Building,

21 97 Lisburn Rd. Belfast, UK BT9 7AE

22 Phone: +44 (0) 28 9097 2260; Fax: +44 (0) 28 9097 2671

23 E-mail: j.bengoechea@qub.ac.uk

24

25 Running title: *Klebsiella* intracellular survival

26

27 **SUMMARY**

28 *Klebsiella pneumoniae* is an important cause of community-acquired and nosocomial  
29 pneumonia. Evidence indicates that *Klebsiella* might be able to persist intracellularly within a  
30 vacuolar compartment. This study was designed to investigate the interaction between  
31 *Klebsiella* and macrophages. Engulfment of *K. pneumoniae* was dependent on host  
32 cytoskeleton, cell plasma membrane lipid rafts and the activation of PI 3-kinase (PI3K).  
33 Microscopy studies revealed that *K. pneumoniae* resides within a vacuolar compartment, the  
34 *Klebsiella* containing vacuolae (KCV), which traffics within vacuoles associated with the  
35 endocytic pathway. In contrast to UV-killed bacteria, the majority of live bacteria did not  
36 colocalize with markers of the lysosomal compartment. Our data suggest that *K. pneumoniae*  
37 triggers a programmed cell death in macrophages displaying features of apoptosis. Our  
38 efforts to identify the mechanism(s) whereby *K. pneumoniae* prevents the fusion of the  
39 lysosomes to the KCV uncovered the central role of the PI3K-Akt-Rab14 axis to control the  
40 phagosome maturation. Our data revealed that the capsule is dispensable for *Klebsiella*  
41 intracellular survival if bacteria were not opsonized. Furthermore, the environment found by  
42 *Klebsiella* within the KCV triggered the downregulation of the expression of *cps*. Altogether,  
43 this study proves evidence that *K. pneumoniae* survives killing by macrophages by  
44 manipulating phagosome maturation which may contribute to *Klebsiella* pathogenesis.

45

## 46 INTRODUCTION

47 In the late nineteenth century, Eli Metchnikoff appreciated phagocytosis as a key process in  
48 the battle against pathogens. Phagocytosis can be conceptually divided into phagosome formation  
49 and its subsequent evolution into a degradative compartment, a process termed phagosome  
50 maturation. This is important because the nascent phagosome is not microbicidal. Maturation not  
51 only aids clearing infection, but also generates and routes antigens for presentation on MHC  
52 molecules in order to activate the adaptive immune system (Trombetta and Mellman. 2005).  
53 Phagosome maturation involves the sequential acquisition of different proteins, many of them of the  
54 endocytic pathway (Vieira *et al.* 2002, Flannagan *et al.* 2012). Thus, during and/or immediately after  
55 phagosome closure, the phagosome fuses with early endosomes, acquiring Rab5 and early  
56 endosome antigen 1 (EEA1). The phagosome rapidly loses the characteristics of early endosome  
57 and acquires late endosome features. The late phagosome is positive for Rab7, the mannose-6-  
58 phosphate receptor, lysobisphosphatidic acid, lysosome-associated membrane proteins (Lamps) and  
59 CD63. Ultimately, the organelle fuses with lysosomes to form the phagolysosome, identified by the  
60 presence of hydrolytic proteases, such as processed cathepsin D, cationic peptides and by an  
61 extremely acidic luminal pH which is regulated primarily by the vacuolar (V-type) ATP-ase  
62 complex. In the course of maturation, an oxidative system formed by the NADPH oxidase and  
63 ancillary proteins is also activated.

64 Many pathogens have developed strategies to counteract the microbicidal action of  
65 macrophages (Flannagan *et al.* 2009, Sarantis and Grinstein. 2012). Some pathogens inhibit  
66 phagocytosis. For example, the role of capsule polysaccharides in preventing opsonophagocytosis  
67 has been appreciated for many pathogens including *Neisseria meningitidis*, *Staphylococcus aureus*  
68 and *streptococci*. Others, such as enteropathogenic *Escherichia coli*, inhibit engulfment by blocking  
69 PI 3-kinase (PI3K) signaling whereas *Yersinia* species inhibits phagocytosis by injecting type III  
70 secretion effectors. Conversely, *Salmonella typhimurium* induces its own uptake and, once inside a  
71 modified phagosome, triggers macrophage death by a caspase-1 dependent process called pyroptosis

72 (Fink and Cookson. 2007). *Brucella* spp. resist an initial macrophage killing to replicate in a  
73 compartment segregated from the endocytic pathway with endoplasmic reticulum properties (von  
74 Bargen *et al.* 2012).

75 *Klebsiella pneumoniae* is a Gram negative capsulated pathogen which causes a wide range  
76 of infections, from urinary tract infections to pneumonia, being particularly devastating among  
77 immunocompromised patients with mortality rates between 25% and 60% (Sahly and Podschun.  
78 1997). *K. pneumoniae* is an important cause of community-acquired pneumonia in individuals with  
79 impaired pulmonary defences and is a major pathogen for nosocomial pneumonia. Pulmonary  
80 infections are often characterized by a rapid clinical course thereby leaving very short time for an  
81 effective antibiotic treatment. *K. pneumoniae* isolates are frequently resistant to multiple antibiotics  
82 (Munoz-Price *et al.* 2013), which leads to a therapeutic dilemma. In turn, this stresses out the  
83 importance of pulmonary innate defense systems to clear *K. pneumoniae* infections.

84 Resident alveolar macrophages play a critical role in the clearance of bacteria from the lung  
85 by their capacity for phagocytosis and killing. It has been shown that depletion of alveolar  
86 macrophages results in reduced killing of *K. pneumoniae in vivo* (Broug-Holub *et al.* 1997, Cheung  
87 *et al.* 2000). This suggests that *Klebsiella* countermeasures against phagocytosis would be  
88 important virulence factors. Supporting this notion, *K. pneumoniae* capsule (CPS) reduces  
89 phagocytosis by neutrophils and macrophages (March *et al.* 2013, Cortes *et al.* 2002b, Regueiro *et al.*  
90 2006, Alvarez *et al.* 2000) and CPS mutant strains are avirulent not being able to cause pneumonia  
91 and urinary tract infections (Cortes *et al.* 2002b, Lawlor *et al.* 2005, Camprubi *et al.* 1993).

92 *K. pneumoniae* has been largely considered as an extracellular pathogen. However, there are  
93 reports showing that *K. pneumoniae* is internalized *in vitro* by different cell types being able to  
94 persist intracellularly for at least 48 h (Oelschlaeger and Tall. 1997). It has been also reported the  
95 presence of intracellular *Klebsiella* spp. within a vacuolar compartment inside human macrophages,  
96 mouse alveolar macrophages and lung epithelial cells *in vivo* (Cortes *et al.* 2002b, Fevre *et al.*  
97 2013, Willingham *et al.* 2009, Greco *et al.* 2012). The present study was designed to investigate the

98 interaction between *K. pneumoniae* and macrophages. We report that *K. pneumoniae* survives  
99 within macrophages by deviating from the canonical endocytic pathway and residing in a unique  
100 intracellular compartment which does not fuse with lysosomes. Mechanistically, our results indicate  
101 that *Klebsiella* targets the PI3K-Akt-Rab14 axis to control the phagosome maturation. Finally, we  
102 present evidence indicating that *K. pneumoniae* has the potential to kill and escape from the  
103 phagocyte.

104

105

## 106 **RESULTS**

### 107 ***K. pneumoniae* survives inside macrophages.**

108 To explore whether *K. pneumoniae* resides inside macrophages *in vivo*, macrophages were  
109 isolated from the bronchoalveolar lavage of mice infected intranasally with *K. pneumonia* strain  
110 43816 (hereafter Kp43816R). Confocal microscopy experiments showed that  $85 \pm 4$  % of the  
111 intracellular bacteria did not colocalize with the lysosomal marker cathepsin D (Fig 1A).  
112 Macrophages isolated obtained from the bronchoalveolar lavage were pulsed-chased with  
113 tetramethylrhodamine-labelled dextran (TR-dextran) as described in the Experimental procedures.  
114 Pulse-chase protocols with TR-dextran are extensively used in the literature to label lysosomes  
115 (Morey *et al.* 2011, Eissenberg *et al.* 1988, Hmama *et al.* 2004, Lamothe *et al.* 2007). Confocal  
116 microscopy revealed that  $80 \pm 3$  % intracellular *Klebsiella* did not colocalize with TR-dextran (Fig  
117 1A).

118 To assess the interaction of *K. pneumoniae* and macrophages in more detail, we standardized  
119 the infection conditions of the mouse macrophage cell line MH-S with Kp43816R. We optimized  
120 the time of bacteria-cell contact (30, 60 and 120 min), the multiplicity of infection (MOI) (100, 50  
121 or 10 bacteria per cell), and the antibiotic treatment necessary to kill the remaining extracellular  
122 bacteria after the contact. To synchronize infection, plates were centrifuged at  $200 \times g$  during 5 min  
123 and intracellular bacteria were enumerated after macrophage lysis with 0.5% saponin in PBS. We  
124 found that 90 min treatment with a combination of gentamicin (300  $\mu\text{g/ml}$ ) and polymyxin B (15

125  $\mu\text{g/ml}$ ) was necessary to kill 99.9% of the extracellular bacteria. The highest numbers of engulfed  
126 bacteria were obtained after 120 min of bacteria-cell contact with a multiplicity of infection (MOI)  
127 of 100:1. However, these conditions also triggered a significant decrease in cell viability as detected  
128 by the trypan blue exclusion method. 30 min of contact and a MOI of 50:1 were the conditions in  
129 which no decrease in cell viability was observed and, therefore, they were used in the subsequent  
130 experiments described in this study.

131 To investigate the molecular mechanisms used by mouse macrophages to engulf Kp43816R,  
132 infections were carried out in the presence of inhibitors of host cell functions (Fig 1B). Cytochalasin  
133 D and nocodazol reduced the engulfment of Kp43816R hence indicating that Kp43816R  
134 phagocytosis requires the assembly of F-actin and the host microtubule network. Methyl- $\beta$ -  
135 cyclodextrin (M $\beta$ CD), which depletes cholesterol from host cell membranes, was employed to  
136 analyse the involvement of lipid rafts in Kp43816R phagocytosis. Cholesterol depletion impaired  
137 *Klebsiella* engulfment by MH-S. Similar results were obtained when cells were treated with filipin  
138 and nystatin (Fig. 1B). Since the generation of phosphoinositides is linked to phagosome formation  
139 (Vieira *et al.* 2001), we assessed the contribution of the PI3K signalling pathway on Kp43816R  
140 phagocytosis. Pre-treatment of MH-S cells with LY294002, a specific inhibitor of PI3K activity,  
141 resulted in the blockage of Kp43816R phagocytosis (Fig. 1B). Immunofluorescence experiments  
142 further confirmed that treatment of cells with LY294002 inhibited the engulfment of *Klebsiella* (Fig  
143 S1). This was also true for UV-killed bacteria (Fig S1). Akt is a downstream effector of PI3K which  
144 becomes phosphorylated upon activation of the PI3K signalling cascade. As expected, western blot  
145 analysis revealed that Kp43816R induces the phosphorylation of Akt in a PI3K-dependent manner  
146 since LY294002 inhibited *Klebsiella*-induced phosphorylation of Akt (Fig. 1C-D). UV-killed  
147 bacteria also induced the phosphorylation of Akt although the levels were significantly lower than  
148 those induced by live bacteria (Fig 1C). The PI3K-Akt cascade is also activated by Kp43816R in  
149 human macrophages (THP-1 monocytes differentiated to macrophages by phorbol-12-myristate-13-  
150 acetate [PMA] treatment; hereafter mTHP-1) (Fig. S2).

151 Bacterial intracellular location in MH-S cells was assessed 3 and 6 h post infection by  
152 transmission electron microscopy (TEM). In good agreement with other published observations *in*  
153 *vivo* (Cortes *et al.* 2002b, Fevre *et al.* 2013, Willingham *et al.* 2009, Greco *et al.* 2012), bacteria were  
154 located in a vacuolar compartment (data not shown). To determine the fate of intracellular  
155 Kp43816R, MH-S cells were infected with GFP-expressing Kp43816R and the number of  
156 intracellular bacteria was assessed microscopically using differential (extracellular/intracellular)  
157 staining and by plating after different incubation times. The number of intracellular bacteria in MH-  
158 S cells decreased during the first 2 h of infection but then it remained constant until 7.5 h post  
159 infection (Fig 2A). Immunofluorescence analysis revealed that the number of infected macrophages  
160 decreased during the first 2 h hence suggesting that some cells are able to clear the infection.  
161 However, after 2 h, the percentage of infected macrophages did not change until the end of the  
162 experiment (Fig 2B). We did not observe any change of host cell morphology (data not shown). The  
163 majority of infected macrophages contained less than three bacteria (Fig 2C). The fact that the  
164 number of macrophages containing between three and five bacteria or more than five did not  
165 change over time suggests that there is not significant bacteria replication. Similar results were  
166 obtained when mTHP-1 cells were infected (Fig S3).

167 To elucidate whether those intracellular bacteria assessed by microscopy were indeed viable,  
168 cells were infected with *Klebsiella* harbouring two plasmids, one conferring constitutive expression  
169 of mCherry (pJT04mCherry) and another one (pMMB207gfp3.1) expressing *gfp* under the control  
170 of an IPTG inducible promoter. Therefore, only metabolically active bacteria will be mCherry-GFP  
171 positive. Microscopy analysis using differential (extracellular/intracellular) staining showed that  
172 more than 75% of intracellular bacteria were mCherry-GFP positive 3.5 h post infection (Fig 2D-E).  
173 This percentage did not change over time. To further confirm that intracellular *Klebsiella* are  
174 metabolically active, fluorescent *in situ* hybridisation (FISH) was carried out by using the  
175 oligonucleotide probes EUB338 and GAM42a (see Experimental procedures). The detection of  
176 bacteria by these oligonucleotide probes is dependent on the presence of sufficient ribosomes per



177 cell, hence providing qualitative information on the physiological state of the bacteria (Christensen  
178 *et al.* 1999, Morey *et al.* 2011). Microscopy analysis revealed that the number of bacteria  
179 metabolically active (FISH positive) *versus* the total number of intracellular bacteria (GFP positive)  
180 was maintained through the infection (Fig. S4).

181 Collectively, these results showed that Kp43816R phagocytosis by macrophages is an event  
182 dependent on host cytoskeleton and cell plasma membrane lipid rafts. Moreover, the PI3K/Akt host  
183 signalling pathway is activated by Kp43816R infection and it is required for bacterial phagocytosis.  
184 Our data demonstrate that Kp43816R survives within macrophages through the course of infection  
185 and the TEM experiments may suggest that Kp43816R may reside in a specific compartment that  
186 we named the *Klebsiella* containing vacuole (KCV).

187

#### 188 ***K. pneumoniae* elicits a cytotoxic effect on macrophages.**

189 Examination of the infected monolayers by immunofluorescence at different time points  
190 revealed a decreased in the overall monolayer density at 10 h post infection which became more  
191 evident 20 h post infection (Fig S5A). This observation prompted us to study whether Kp43816R  
192 exerts a cytotoxic effect on macrophages. We assessed the viability of infected MH-S cells by  
193 measuring the levels of LDH release. Kp43816R infection was associated with a 35% decrease in  
194 cell viability after 20 h of infection. Kp43816R-triggered cytotoxic effect on macrophages was also  
195 evident when cell viability was estimated by the neutral red uptake assay (Fig S5B).

196 The induction of host cell apoptosis is one mechanism used by some pathogens to augment  
197 infection (Navarre and Zychlinsky. 2000). To test whether Kp43816R causes apoptosis of MH-S  
198 cells, apoptosis was measured with annexin V, to analyze phosphatidylserine translocation to the  
199 outer leaflet of the plasma membrane, and 7-actinomycin D (AAD) to evaluate plasma membrane  
200 integrity. Flow cytometry analysis of infected cells showed a significant increased in annexin  
201 V<sup>+</sup>AAD<sup>-</sup> cells over time (Fig. 3). The amount of double-positive annexinV<sup>+</sup>AAD<sup>+</sup> cells, which  
202 corresponds to a necrotic-like phenotype, was markedly lower than the amount of cells annexin

203  $V^+AAD^-$  at all times analyzed. These results indicate phosphatidylserine translocation and intact  
204 membrane integrity, a classical apoptotic phenotype, hence suggesting that Kp43816R triggers  
205 apoptosis in macrophages.

206

207 ***K. pneumoniae* prevents phagosome fusion with lysosomes.**

208       Because Kp43816R is able to survive within macrophages, we hypothesized that *Klebsiella*  
209 must either divert the normal process of phagosome maturation or withstand the hostile  
210 environment of the mature phagolysosome. Therefore, we analyzed the maturation of the KCV  
211 during the course of an infection by unravelling the association of the KCV with compartments of  
212 the exocytic and endocytic pathways. Bacteria did not colocalize with either markers of the  
213 endoplasmic reticulum (calnexin) or markers of the Golgi network (GM 130) at any time point  
214 analyzed (Fig S6). EEA1 is an early endosome-specific peripheral membrane protein which  
215 colocalizes with the small GTP binding protein Rab5 (Vieira *et al.* 2002, Flannagan *et al.* 2012). As  
216 shown in Figure 4, we could detect the presence of EEA1 on  $22 \pm 4\%$  of KCVs at 15 min post  
217 infection. The percentage of vacuoles positive for this marker dropped to  $15 \pm 9\%$  and to  $5 \pm 1\%$  at  
218 60 and 90 min post infection, respectively (Fig 4). We next sought to determine whether the KCV  
219 acquires the late endosomal markers Lamp1 and Rab7 (Vieira *et al.* 2002, Flannagan *et al.* 2012).  
220 KCVs were positive for Lamp1 already at 15 min post infection and the percentage of positive  
221 KCVs increased over time (Fig 4). KCVs remained positive for Lamp1 until 7.5 h post infection.  
222 Rab7 is a small GTPase that controls vesicular transport to late endosomes and lysosomes in the  
223 endocytic pathway (Rink *et al.* 2005). To assess the presence of Rab7 on KCVs, macrophages were  
224 transfected with GFP-Rab7 and then infected with Kp43816R. The majority of the vacuoles  
225 containing Kp43816R were positive for both Rab7 and Lamp1 (Fig 4). To determine the activation  
226 status of Rab7 we asked whether RILP, a Rab7 effector protein that exclusively recognizes the  
227 active (GTP bound) conformation of Rab7 (Cantalupo *et al.* 2001, Jordens *et al.* 2001), labels the  
228 KCV. Before infection, cells were transfected with a plasmid containing GFP fused to the C-

terminal Rab7-binding domain of RILP, called “RILP-C33”, which can be used as a reliable index of the presence and distribution of active Rab7 (Cantalupo *et al.* 2001, Jordens *et al.* 2001). As shown in Figure 4 RILP-C33-EGFP colocalized with the majority of KCVs. These vacuoles were also positive for Lamp1.

Since the interaction of Rab7 with RILP drives fusion with lysosomes (Cantalupo *et al.* 2001, Jordens *et al.* 2001), we sought to determine whether KCV colocalizes with lysosomal markers. Although there are not markers that unambiguously distinguish late endosomes from lysosomes, mounting evidence indicates that an acidic luminal pH and the presence of hydrolytic proteases, such as processed cathepsin D, are characteristics of the phagolysosomal fusion (Vieira *et al.* 2002, Flannagan *et al.* 2012). We used the fixable acidotropic probe LysoTracker to monitor acidic organelles in infected macrophages. We found a major overlap between the dye and the KCVs (Fig 5), hence indicating that the KCV is acidic. We next examined the presence in the vacuole of cathepsin D as a marker for the lysosomal soluble content. The majority of the KCVs did not colocalize with cathepsin D (Fig 5), thereby suggesting that the KCV does not fuse with lysosomes. To further sustain this notion, we assessed KCV colocalization with TR-dextran. Prior to bacterial infection macrophages were pulsed with TR-dextran for 2 h followed by a 1 h chase in dye-free medium to ensure that the probe is delivered from early and recycling endosomes to phagolysosomes (Morey *et al.* 2011, Eissenberg *et al.* 1988, Hmama *et al.* 2004, Lamothe *et al.* 2007). Confocal immunofluorescence showed that the majority of the KCVs did not colocalize with TR-dextran (Fig 5B). In contrast, when macrophages were infected with UV-killed Kp43816R more than 70% of the KCVs did colocalize with cathepsin D and TR-dextran 1.5 h post infection (Fig S7). Collectively, these results strongly support the notion that the majority of KCVs containing live bacteria prevent the fusion of the vacuole with lysosomes.

Similar findings were obtained when mTHP-1 cells were infected. KCV was not associated with compartments of the exocytic pathway, either Golgi network or endoplasmic reticulum, but acquired markers of the endocytic pathway, EEA1 and Lamp1 (Fig S8A). The majority of KCVs

255 colocalized with LysoTracker (Fig S8A) but they were negative for cathepsin D (Fig S8B). In  
256 contrast, nearly 70% of UV-killed Kp43816R colocalized with cathepsin D after 2 h post infection  
257 (Fig S8B). Altogether, these results indicate that only phagosomes containing UV-killed *Klebsiella*  
258 bacteria fuse with lysosomes in human macrophages.

259 In summary, these findings suggest that *K. pneumoniae* trafficks inside macrophages within  
260 vacuoles associated to the endocytic pathway, and that live bacteria perturb the fusion of the KCV  
261 with the hydrolases-rich lysosomal compartment.

262

### 263 **Inhibition of compartment acidification affects *K. pneumoniae* intracellular survival.**

264 Phagosome acidification has been shown to be essential for the intracellular survival of  
265 several pathogens (Morey *et al.* 2011, Ghigo *et al.* 2002, Porte *et al.* 1999). Therefore, we  
266 investigated the effect of inhibiting KCV acidification on *K. pneumoniae* survival. Bafilomycin A<sub>1</sub>  
267 is a specific inhibitor of the vacuolar type H<sup>+</sup>-ATPase in cells, and inhibits the acidification of  
268 organelles containing this enzyme, such as lysosomes and endosomes. As expected,  
269 phagolysosomal acidification was sensitive to bafilomycin A<sub>1</sub> treatment (Fig 6A), hence confirming  
270 dependence on the vacuolar H<sup>+</sup>-ATPase. Moreover, bafilomycin A<sub>1</sub> treatment also abrogated the  
271 overlap between Kp43816R and the probe LysoTracker (Fig 6A). To assess the effect of vacuolar  
272 acidification on Kp43816R survival, cells were treated with bafilomycin A<sub>1</sub> at the onset of the  
273 gentamicin treatment and bacteria were enumerated by plating at different time points. Data shown  
274 in Figure 6C revealed that the number of intracellular Kp43816R decreased in bafilomycin A<sub>1</sub>  
275 treated cells over time compared to infected untreated cells. Control experiments revealed that  
276 bafilomycin A<sub>1</sub> has no toxic effect on *K. pneumoniae* (our control experiments [data not shown]) or  
277 on other Gram-negative bacteria (Morey *et al.* 2011, Porte *et al.* 1999). Microscopy analysis  
278 revealed that the percentages of Kp43186R colocalization with TR-dextran in bafilomycin A<sub>1</sub>  
279 treated cells either at 3.5 or 5.5 h post infection (19 ± 4 and 20 ± 5%, respectively) were similar to  
280 those in DMSO (vehicle solution)-treated cells (20 ± 4 and 24 ± 6 %, respectively). In turn, the

percentage of mCherry-GFP positive intracellular bacteria dropped from  $85 \pm 7$  % in DMSO-treated cells to  $25 \pm 4$  % in bafilomycin A<sub>1</sub> treated cells already at 2.5 h post infection ( $P < 0.05$  Mann-Whitney U test). Altogether, these observations suggest that Kp43816R intracellular survival requires KCV acidification.

### **PI3K-AKT and Rab14 contribute to *K. pneumoniae* intracellular survival.**

*S. enterica* serovar *typhimurium* perturbs the fusion of the phagosomes with lysosomes by activating the host kinase Akt (Kuijl *et al.* 2007). In turn, inhibition of Akt activation reduces *Salmonella* intracellular survival (Kuijl *et al.* 2007, Chiu *et al.* 2009). Several pathogens also target the PI3K-Akt axis to manipulate cell biology for their own benefit (Krachler *et al.* 2011). Since Kp43816R induced the activation of Akt in a PI3K-dependent manner we sought to determine the contribution of the PI3K-Akt axis to the intracellular survival of *K. pneumoniae*. Treatment of cells with the PI3K inhibitor LY294002 or the Akt inhibitor AKT X at the onset of the gentamicin treatment reduced the number of intracellular bacteria in MH-S cells (Fig 7A). Moreover, microscopy analysis revealed that more than 70% bacteria colocalized with either TR-dextran or cathepsin D in cells treated with AKT X (Fig 7B and Fig S9). Collectively, these results support the notion that Kp43816R targets the PI3K-Akt axis to survive intracellularly.

At least 18 Rab GTPases are implicated in phagosomal maturation (Smith *et al.* 2007). Interestingly, *Salmonella* targets Rab14 to prevent phagosomal maturation in an Akt dependent manner (Kuijl *et al.* 2007). We speculated that Kp43816R may also target Rab14 to control the maturation of the phagosome. Immunofluorescence experiments revealed that GFP-Rab14 colocalized with the KCVs (Fig 7C-D). To determine whether Rab14recruitment is required for intracellular survival, cells were transfected with a Rab14 dominant-negative construct (DN-Rab14) or control vector and then infected with Kp43816R. As shown in figure 7E, we found a 60% decrease in the number of intracellular bacteria in cells transfected with DN-Rab14. Supporting that *Klebsiella* recruited Rab14 to the KVC in an Akt-dependent manner, GFP-Rab14 did not colocalize

307 with the KCV in AKT X treated cells ( $7 \pm 2$  % percentage of colocalization at 2.5 h post infection)  
308 (Fig 7F).

309 In summary, our results are consistent with a model where Kp43816R targets the PI3K-Akt-  
310 Rab14 axis to control the phagosome maturation to survive inside macrophages.

311

### 312 ***K. pneumoniae* capsule polysaccharide is dispensable for intracellular survival.**

313 We were keen to identify *K. pneumoniae* factors necessary for intracellular survival. Given  
314 the importance of *K. pneumoniae* CPS on host-pathogen interactions, we explored whether CPS is  
315 also necessary for *K. pneumoniae* intracellular survival. As anticipated, a CPS mutant was engulfed  
316 by MH-S and mTHP1 macrophages in higher numbers than Kp43816R (data not shown). For the  
317 sake of comparison with the wild-type strain in time-course experiments, we adjusted the MOI of  
318 the CPS mutant to get comparable numbers of intracellular bacteria at the beginning of the  
319 infection. Time course experiments showed no differences between the number of intracellular  
320 bacteria of both strains in MH-S and mTHP1 cells (Fig 8A).

321 Given the critical role of CPS in preventing complement-mediated opsonophagocytosis  
322 (Alvarez *et al.* 2000, de Astorza *et al.* 2004, Cortes *et al.* 2002a), we evaluated whether the  
323 intracellular fate of the CPS mutant could be modified by bacterial opsonization with human serum.  
324 In agreement with previous reports (de Astorza *et al.* 2004, Cortes *et al.* 2002a), opsonization of the  
325 CPS mutant resulted in an increase in the number of ingested bacteria by mTHP1 cells compared to  
326 nonopsonized bacteria (Fig 8B). For the sake of comparison, the MOI was adjusted to get  
327 comparable numbers of intracellular bacteria at the beginning of the infection. The number of CFU  
328 recovered from cells infected with the opsonized CPS mutant was significantly lower than the  
329 number of CFU recovered from cells infected with non-opsonized bacteria (100 fold lower at 8 h  
330 post infection; Fig 8C). These data indicate that internalization via the C3 receptor results in a  
331 significant loss of intracellular viability, presumably because these bacteria are ultimately delivered  
332 to lysosomes.

333       The lack of contribution of CPS to intracellular survival prompted us to analyze the  
334 expression of *cps* in the KCV. To monitor *cps* expression over time, we generated a transcriptional  
335 fusion in which the *cps* promoter region was cloned upstream a promoterless *gfp* that encodes a  
336 protein tagged at the C terminus with the (LVA) peptide. The GFP(LVA) protein is targeted for Tsp  
337 protease degradation within the bacteria and has been reported to have 40-min half-life, while  
338 untagged GFP is very stable (estimated *in vivo* half-life, 24 h) (Miller *et al.* 2000). We assessed  
339 GFP fluorescence in Kp43816R containing the unstable GFP reporter grown in LB. *Klebsiella* was  
340 stained using rabbit anti-*Klebsiella* serum followed by Rhodamine-conjugated donkey anti-rabbit  
341 secondary antibody. FACS analysis revealed an overlap between GFP fluorescence (green  
342 histogram) and Rhodamine fluorescence (red histogram) in bacteria grown in LB (Fig 8D, panel  
343 label as inoculum) which is in perfect agreement with the constitutive expression of *cps* by bacteria  
344 grown in LB. To investigate *cps* expression in intracellular bacteria, MH-S cells were infected with  
345 Kp43816R containing the GFP reporter. Cells were processed as described in Experimental  
346 procedures, and fluorescence analysed by FACS at different time points post infection. GFP  
347 fluorescence (green histograms) was measured in the gated Rhodamine positive population (red  
348 histograms). Data in Figure 8D shows that GFP fluorescence decreased over time in the  
349 intracellular bacteria reaching the levels of the control strain carrying the empty vector (grey  
350 histogram), which is considered negative for GFP fluorescence.

351       To explore whether the acidic pH of the KCV might be responsible for the downregulation  
352 of *cps* expression, bacteria were grown in M9 minimal medium, with 8  $\mu$ M magnesium sulfate,  
353 buffered to different pHs. The expression of the *cps::gfp* fusion was 5-fold lower when bacteria  
354 were grown at pH 5.5 than at pH 7.5 (Fig 8E). Similar results were obtained when the mRNA levels  
355 of *wzi*, *orf7* and *gnd*, three genes of the *cps* operon (Arakawa *et al.* 1995), were assessed by real  
356 time quantitative PCR (RT-qPCR) (Fig 8F).

357       Collectively, these findings show that *K. pneumoniae* CPS is dispensable for intracellular  
358 survival. In fact, the environment found by *Klebsiella* within the KCV triggers the downregulation

359 of the expression of *cps*. The fact that opsonization affects the intracellular survival of the CPS  
360 mutant indicates that the mechanism of bacteria entry into macrophages has a major impact in the  
361 ability of *K. pneumoniae* to survive intracellularly.

362

## 363 **DISCUSSION**

364 In this work, we present compelling evidence demonstrating that *K. pneumoniae* survives  
365 killing by macrophages by manipulating phagosome maturation. Our data sustain that *K.*  
366 *pneumoniae* traffics within vacuoles associated with the endocytic pathway in mouse and human  
367 macrophages. In contrast to UV-killed bacteria, which colocalize with lysosomal markers, live  
368 bacteria modify the vacuole biogenesis preventing the fusion of the KCV with the hydrolases-rich  
369 lysosomal compartment. *K. pneumoniae* thus increases the list of pathogens able to alter phagosome  
370 maturation.

371 Engulfment of *K. pneumoniae* by mouse and human macrophages was dependent on host  
372 cytoskeleton, cell plasma membrane lipid rafts and the activation of PI3K which are all commonly  
373 needed to engulf pathogens and inert particles such as latex beads (Vieira *et al.* 2002, Flannagan *et*  
374 *al.* 2012). TEM analysis suggested that *K. pneumoniae* resides inside a vacuolar compartment and,  
375 by using FISH and two fluorescent markers tagging, we confirmed that intracellular bacteria are  
376 metabolically active. Several lines of evidence indicate that *K. pneumoniae* infections are associated  
377 with cell death (Willingham *et al.* 2009, Cano *et al.* 2009, Cai *et al.* 2012). In good agreement, in this  
378 study we show that *K. pneumoniae* triggers a programmed cell death in macrophages displaying  
379 features of apoptosis. Of note, kinase activity profiling in whole lungs during *K. pneumoniae*  
380 infection showed the activation of kinases associated to induction of apoptosis (Hoogendijk *et al.*  
381 2011). However, Willingham and co-workers reported that *K. pneumoniae* activates the NLRP3-  
382 dependent cell death programme termed pyronecrosis (Willingham *et al.* 2009). Similar apparently  
383 contradictory findings have been reported for *Shigella flexneri* infections. *Shigella* triggers  
384 apoptotic and pyroptotic cell death in macrophages depending on the bacterial dosage and time of



385 infection (Willingham *et al.* 2007,Hilbi *et al.* 1998). In that case, short time of bacteria-cell contact  
386 and low MOI are associated to induction of apoptosis (Willingham *et al.* 2007,Hilbi *et al.* 1998).  
387 Notably, the infection conditions in our study are different to those used by Willingham and co-  
388 workers who used a MOI four times higher than ours (Willingham *et al.* 2009). Future studies are  
389 warranted to carefully assess the influence of infection conditions on *Klebsiella*-induced cell death.

390 Manipulation of cell death is a common pathogenic strategy not only for bacteria but also for  
391 viruses (Finlay and McFadden. 2006). In general, viruses either accelerate or inhibit apoptosis of  
392 the infected cell, depending on the biology of the specific virus. Like viruses, obligate intracellular  
393 bacteria generally suppress apoptotic death. Because apoptosis is a less inflammatory process than  
394 necrotic death, many nonobligate intracellular pathogens trigger apoptotic death to avoid cell to cell  
395 communications. Thus, *Klebsiella*-induced macrophage death by apoptosis could be considered a  
396 central aspect of *Klebsiella* infection biology taken into account the evidence demonstrating that  
397 alveolar macrophages play a critical role in the clearance of *Klebsiella* (Broug-Holub *et al.*  
398 1997,Cheung *et al.* 2000) and the importance of an early inflammatory responses to control the  
399 infection (Greenberger *et al.* 1996a,Greenberger *et al.* 1996b,Happel *et al.* 2005,Happel *et al.*  
400 2003).

401 The vacuole of *K. pneumoniae* and its biogenesis was studied by immunofluorescence. The  
402 presence of EEA1 on the KCV indicates that internalized bacteria are initially present in a vacuole  
403 related to the endocytic pathway. However, *K. pneumoniae* does not remain in early endosomes as  
404 demonstrated by the acquisition of Lamp1 and Rab7. A hallmark of the maturation is the exclusion  
405 of lysosomal hydrolases in the majority of KCVs containing live bacteria. In contrast, more than  
406 50% of the KCVs containing UV-killed bacteria were positive for lysosomal markers already 90  
407 min post infection. The KCV is acidic most likely due to the activity of vacuolar proton-ATPases.  
408 Notably, inhibition of these pumps by bafilomycin A<sub>1</sub> resulted in a decrease in intracellular  
409 bacterial numbers. Similar findings have been reported for non typable *H. influenzae*, *Tropheryma*  
410 *whipplei*, and *Brucella suis* (Morey *et al.* 2011,Ghigo *et al.* 2002,Porte *et al.* 1999). The reduction

411 of intracellular viability may have several explanations. Bafilomycin A<sub>1</sub> might affect other  
412 macrophage functions necessary for *K. pneumoniae* survival. An alternative hypothesis, and more  
413 appealing to us, is that *K. pneumoniae* requires a low pH environment for survival within the KCV  
414 which is in agreement with our data showing a significant decrease in the number of metabolic  
415 active intracellular bacteria in bafilomycin A<sub>1</sub>-treated cells. For example, the acidic environment  
416 may facilitate the uptake of nutrients by *Klebsiella*. Acidic pH is required for the transport of  
417 glucose in *Coxiella burnetii* (Howe and Mallavia. 2000) and localization in an acidic environment  
418 facilitates the availability of iron for the growth of *Francisella tularensis* (Fortier *et al.* 1995). In  
419 addition, low pH may regulate the expression of factors essential for intracellular survival. This has  
420 been shown to be true for virulence gene transcription in *S. typhimurium* (Yu *et al.* 2010). In this  
421 context, our data revealed that *Klebsiella* downregulates the expression of *cps* when residing within  
422 the KCV. Interestingly, when *Klebsiella* was cultured in low magnesium and acidic pH we also  
423 found a downregulation of *cps* expression. It is tempting to speculate that these signals could trigger  
424 *cps* downregulation within the KCV. In fact, we show here that the KCV is acidic and there are  
425 reports suggesting that the magnesium concentration in pathogen-containing vacuoles is in the  
426 micromolar range (Garcia-del Portillo *et al.* 1992). Future efforts will be devoted to characterize the  
427 chemical composition of the KCV as well as the transcriptional landscape of intracellular *K.*  
428 *pneumoniae*.

429         It was interesting to consider the mechanism(s) whereby *K. pneumoniae* prevents the fusion  
430 of the lysosomes to the KCV. The overall resemblance between the KCV and the *Salmonella*  
431 containing vacuole (acidic Lamp-1-positive cathepsin-negative vacuole) prompted us to explore  
432 whether *K. pneumoniae* employs similar strategies as *Salmonella* to subvert phagosome maturation.  
433 Kuijl and coworkers (Kuijl *et al.* 2007) demonstrated that *S. typhimurium* activates Akt to prevent  
434 phagosome-lysosome fusion. Since *K. pneumoniae* activates Akt *in vitro* (this work and (Frank *et*  
435 *al.* 2013)) and *in vivo* (Hoogendijk *et al.* 2011) we speculated that activated Akt may also promote  
436 *Klebsiella* intracellular survival. Indeed this was the case. Akt inhibition resulted in a significant

437 decrease in bacterial intracellular survival associated with an increased colocalization of the KCV  
438 with lysosomal markers. The fact that Akt is implicated in the intracellular survival of other  
439 pathogens, including *M. tuberculosis* (Kuijl *et al.* 2007), strongly suggests that this kinase is a  
440 central host node targeted by pathogens to take control over cellular functions.

441 PI3K/Akt governs phagosome maturation by controlling, at least, the activation of Rab  
442 GTPases (Thi and Reiner. 2012), although Rab14 is emerging as a central Rab in this process.  
443 Previous data indicate that pathogens hijack Rab14 to manipulate phagosome maturation. The *M.*  
444 *tuberculosis* vacuole recruits and retains Rab14 to maintain early endosomal characteristics (Kyei *et*  
445 *al.* 2006) whereas *S. typhimurium* containing vacuole retains Rab14 in an Akt-dependent manner to  
446 arrest phagosome maturation (Kuijl *et al.* 2007). Immunofluorescence confirmed that the KCV is  
447 positive for Rab14 in an Akt-dependent manner whereas transient transfection of the dominant-  
448 negative Rab14 resulted in a decrease in bacteria intracellular survival. In aggregate, this evidence  
449 supports a scenario in which *K. pneumoniae* manipulates phagosome maturation by targeting a  
450 PI3K-Akt-Rab14 pathway. Nevertheless, we do not rule out that there are additional pathways  
451 necessary for *Klebsiella* intracellular survival.

452 We were keen to identify the bacterial factors interfering with the phagosomal maturation  
453 pathway. Given the critical role of *K. pneumoniae* CPS in preventing host defense responses (March  
454 *et al.* 2013, Regueiro *et al.* 2006, Lawlor *et al.* 2005, Frank *et al.* 2013, Moranta *et al.* 2010, Campos *et*  
455 *al.* 2004, Lawlor *et al.* 2006), we hypothesized that CPS is necessary for intracellular survival. To  
456 our initial surprise, CPS does not play a large role, if any, in intracellular survival of *Klebsiella*  
457 since a *cps* mutant did not display any loss of viability upon phagocytosis. Furthermore, the *cps*  
458 mutant also triggered a programmed cell death in macrophages (data not shown). At first glance,  
459 these findings may seem contradictory with the well-established role of CPS in *K. pneumoniae*  
460 virulence. However, considering the presence of complement in the bronchoalveolar fluid (Wu *et*  
461 *al.* 2005), the fact that opsonization results in more efficient internalization of pathogens and  
462 maturation of phagosomes (Aderem and Underhill. 1999), and the well-known role of CPS in

463 preventing complement opsonization (de Astorza *et al.* 2004,Cortes *et al.* 2002a), we hypothesized  
464 that the *cps* mutant opsonization is deleterious to its intracellular fate. Indeed, this was the case  
465 hence revealing the critical role of CPS on *Klebsiella*-macrophage interplay. These results also  
466 illustrate how the mode of entry of a pathogen influences its intracellular outcome. Similar findings  
467 have been reported for other pathogens (Geier and Celli. 2011,Gordon *et al.* 2000,Drevets *et al.*  
468 1993) but it cannot be considered a general feature since complement opsonization does not affect  
469 the intracellular fate of *Salmonella* and *M. tuberculosis* (Drecktrah *et al.* 2006,Zimmerli *et al.*  
470 1996).

471 At present we can only speculate why *Klebsiella* downregulates the expression of *cps* once  
472 inside the KCV. Since CPS biosynthesis is a metabolically demanding process, *Klebsiella* may  
473 downregulate *cps* expression to better survive in the intracellular environment poor in nutrients. It  
474 is also plausible that CPS may interfere with *Klebsiella* factors implicated in the intracellular  
475 survival. Current efforts of the laboratory are devoted to identify these factors.

476 Finally, it is worthwhile commenting on the clinical implications of this study. The  
477 antibiotics commonly used to treat *Klebsiella* infections are not very efficient against intracellular  
478 bacteria. In turn, our findings provide rationale for the use of inhibitors targeting the PI3K-Akt  
479 signaling cascade to eliminate intracellular *K. pneumoniae*. The concept of eradicating pathogens  
480 through targeting host factors modulated by pathogens has received wide attention in the infectious  
481 disease arena. Several promising drugs have been developed or are being developed to antagonize  
482 PI3K/Akt due to its relevance for many human cancers. Of note, there are *in vitro* and *in vivo*  
483 studies supporting the use of Akt inhibitors to eliminate intracellular *Salmonella* and *M.*  
484 *tuberculosis* (Kuijl *et al.* 2007,Chiu *et al.* 2009). Therefore, we propose that agents targeting  
485 PI3K/Akt might provide selective alternatives to manage *K. pneumoniae* pneumonias. Careful  
486 designed preclinical trials using the well establish mouse pneumonia model are warranted to test  
487 this hypothesis.

488

## 489 **EXPERIMENTAL PROCEDURES**

### 490 **Bacterial strains and growth conditions.**

491 Kp43816R is a rifampicin-resistant derivative of *K. pneumoniae* pneumonia clinical isolate  
492 [ATCC 43816; (Bakker-Woudenberg *et al.* 1985)]. This strain has been widely used to study the  
493 host response to Gram-negative pneumonia because it recapitulates acute pneumonia with fatal  
494 systemic spread at a relatively low infectious dose. Kp43816R expresses a type 1 O-polysaccharide  
495 and a type 2 capsule. Bacteria were grown in lysogeny broth (LB) at 37°C on an orbital shaker (180  
496 rpm). To UV kill bacteria, samples were UV irradiated (1 joule for 15 min) in a BIO-LINK BLX  
497 crosslinker (Vilber Lourmat). When appropriate, antibiotics were added to the growth medium at  
498 the following concentrations: rifampicin (Rif) 50 µg/ml, ampicillin (Amp), 100 µg/ml for *K.*  
499 *pneumoniae* and 50 µg/ml for *E. coli*; kanamycin (Km) 100 µg/ml; chloramphenicol (Cm) 12.5  
500 µg/ml.

### 501 **Construction of a *K. pneumoniae* *cps* mutant.**

502 Primers for *manC* mutant construction were designed from the known *K. pneumoniae* K2  
503 gene cluster sequence (Arakawa *et al.* 1995). Primer pairs ManCUPF (5'-  
504 CGCTTAAAGACCAGCGTGTCTG -3'), ManCUPR (5'-  
505 CCGATCCGATCAGCGGGTCGTCGCCGTG\_\_\_\_-3'), and ManCDOWNF (5'-  
506 CCGATCCGCAGCGACGAGAAGCTGGTGG-3' *Bam*HI site underlined), ManCDOWNR (5'-  
507 GGATATCCCGCAGGCCGGTG -3') were used in two sets of asymmetric PCRs to obtain DNA  
508 fragments ManCUP and ManCDown, respectively. DNA fragments ManCUP and ManCDOWN  
509 were annealed at their overlapping region and amplified by PCR as a single fragment using primers  
510 ManCUPF and ManCDOWNR. This PCR fragment was cloned into pGEM-T Easy to obtain  
511 pGEMTΔ*manC*. A kanamycin cassette, obtained as a 1.5 kb PCR fragment from pKD4 (Datsenko  
512 and Wanner. 2000) using primers cassette-F1 (5'-  
513 CGCGGATCCGTGTAGGCTGGAGCTGCTTCG-3' *Bam*HI site underlined) and cassette-R1 (5'-  
514 CGCGGATCCCATGGGAATTAGCCATGGTCC -3' *Bam*HI site underlined), was BamHI-

515 digested and cloned into BamHI-digested pGEMT $\Delta$ manC to obtain pGEMT $\Delta$ manCKm. Primers  
516 ManCUPF and ManCDOWNR were used to amplify a 3.5 kb fragment which was electroporated  
517 into Kp43816R containing pKOBEG-sacB plasmid (Derbise *et al.* 2003). The vector pKOBEG-  
518 sacB contains the Red operon expressed under the control of the arabinose inducible pBAD  
519 promoter and the sacB gene that is necessary to cure the plasmid. A recombinant in which the wild-  
520 type allele was replaced by  $\Delta$ man::Km was verified by PCR and named 43 $\Delta$ manCKm. The mutant  
521 was resistant to the CPS-specific phage  $\phi$ 2.

## 522 **Eukaryotic cells culture.**

523 Murine alveolar macrophages MH-S (ATCC, CRL-2019) and human monocytes THP-1  
524 (ATCC, TIB-202) were grown in RPMI 1640 tissue culture medium supplemented with 10% heat-  
525 inactivated fetal calf serum (FCS) and 10 mM Hepes at 37°C in an humidified 5% CO<sub>2</sub> atmosphere.  
526 THP-1 cells were differentiated to macrophages by PMA-treatment (10 ng/ml for 12 h).

## 527 **Infection of macrophages.**

528 Macrophages were seeded in 24-well tissue culture plates at a density of  $7 \times 10^5$  cells per  
529 well 15 h before the experiment. Bacteria were grown in 5-ml LB, harvested in the exponential  
530 phase ( $2500 \times g$ , 20 min, 24°C), washed once with PBS and a suspension containing approximately  
531  $1 \times 10^9$  cfu/ml was prepared in 10 mM PBS (pH 6.5). Cells were infected with 35  $\mu$ l of this  
532 suspension to get a multiplicity of infection of 50:1 in a final volume of 500  $\mu$ l RPMI 1640 tissue  
533 culture medium supplemented with 10% heat-inactivated FCS and 10 mM Hepes. To synchronize  
534 infection, plates were centrifuged at  $200 \times g$  during 5 min. Plates were incubated at 37°C in a  
535 humidified 5% CO<sub>2</sub> atmosphere. After 30 min of contact, cells were washed twice with PBS and  
536 incubated for additional 90 min with 500  $\mu$ l RPMI 1640 containing 10% FCS, 10 mM Hepes,  
537 gentamicin (300  $\mu$ g/ml) and polymyxin B (15  $\mu$ g/ml) to eliminate extracellular bacteria. This  
538 treatment did not induce any cytotoxic effect which was verified measuring the release of lactate  
539 dehydrogenase (LDH) and by immunofluorescence microscopy (data not shown). For time course

540 experiments, after the 90 min treatment period, cells were washed three times with PBS and  
541 incubated with 500 µl RPMI 1640 containing 10% FCS, 10 mM Hepes, gentamicin (100 µg/ml).

542 To determine intracellular bacterial load, cells were washed three times with PBS and lysed  
543 with 300 µl of 0.5% saponin in PBS for 10 min at room temperature. Serial dilutions were plated on  
544 LB to quantify the number of intracellular bacteria. Intracellular bacterial load is represented as cfu  
545 per well. All experiments were done with triplicate samples on at least three independent occasions.

546 When indicated, cells were pre-incubated for 1 h with nocodazole (50 µg/ml), filipin (5  
547 µg/ml), nystatin (25 µg/ml), LY294002 hydrochloride (75µM), or for 30 min with cytochalasin D  
548 (5 µg/ml) before carrying out infections as described above. Cells were also pre-incubated for 1 h  
549 with 1 mM methyl-β-cyclodextrin (MβCD), washed twice with PBS to remove cholesterol and  
550 infected. In other experiments, LY294002 hydrochloride (75µM), AKT X (10 µM), or 100 nM  
551 bafilomycin A<sub>1</sub> were added to the cells during the gentamicin treatment and kept until the end of  
552 experiment. Exposure to these drugs had no effect on cell and bacterial viability under the  
553 conditions tested. All drugs were purchased from Sigma.

#### 554 **Immunofluorescence and transmission electron microscopy.**

555 Cells were seeded on 12 mm circular coverslips in 24-well tissue culture plates. Infections  
556 were carried out as described before with *K. pneumoniae* strains harbouring pFPV25.1Cm (March  
557 *et al.* 2013). Control experiments showed that there were no differences in the number of  
558 intracellular bacteria recovered over time from cells infected with bacteria containing pFPV25.1Cm  
559 or no plasmid (data not shown). When indicated, cells were washed three times with PBS and fixed  
560 with 3% paraformaldehyde (PFA) in PBS pH 7.4 for 15 min at room temperature. For EEA1  
561 staining, cells were fixed with 2.5% PFA for 10 min at room temperature followed by 5% PFA +  
562 methanol (1:4 v/v) at -20°C for 5 min. Methanol fixation (3% PFA for 20 min at room temperature  
563 followed by 1 min cold methanol) was used for cathepsin D whereas periodate-lysine-  
564 paraformaldehyde fixation (0.01 M NaIO<sub>4</sub>, 0.075 M L-lysine, 0.0375 M NaPO<sub>4</sub> buffer pH 7.4, 2%  
565 paraformaldehyde: 20 min room temperature) was used for calnexin. The actin cytoskeleton was

566 stained with Rhodamine-Phalloidin (Invitrogen) diluted 1:100, DNA was stained with Hoechst  
567 33342 (Invitrogen) diluted 1:2500. *Klebsiella* was stained with rabbit anti-*Klebsiella* serum diluted  
568 1:5000. Early endosomes were stained with goat anti-EEA1 (N-19) antibody (Santa Cruz  
569 Biotechnology) diluted 1:50. Late endosomes were stained with rat anti-Lamp-1 (1D4B) antibody  
570 (Developmental Studies Hybridoma Bank). Lysosomes were labelled with goat anti-human  
571 cathepsin D (G19) or rabbit anti-human cathepsin D (H-75) antibodies (Santa Cruz Biotechnology)  
572 diluted 1:100. Golgi network was stained with mouse anti-GM130 (BD Laboratories) diluted 1:400.  
573 Endoplasmic reticulum was stained with rabbit anti-calnexin (SPA-860; Enzo Life Sciences) diluted  
574 1:400. Donkey anti-rabbit, donkey anti-mouse, donkey anti-rat and donkey anti-goat conjugated to  
575 Rhodamine, Cy5 or Cy2 secondary antibodies were purchased from Jackson Immunological and  
576 diluted 1:200. Donkey anti-rabbit conjugated to AlexFluor 595 and goat anti-rabbit conjugated to  
577 Cascade blue antibodies (Life technologies) were diluted 1:200.

578         Fixable dextran 70,000 (molecular weight) labelled with Texas red (TR-dextran) (Molecular  
579 Probes) was used to label lysosomes in a pulse-chase assay. Briefly, macrophages seeded on glass  
580 coverslips were labelled by pulsing with 250 µg/ml of TR-dextran for 2 h at 37°C in 5% CO<sub>2</sub> in  
581 RPMI 1640 medium. To allow TR-dextran to accumulate in lysosomes, medium was removed; cells  
582 were washed three times with PBS, and incubated for 1 h in dye-free medium (chase). After the  
583 chase period, cells were infected.

584         LysoTracker Red DND-99 (Invitrogen) was used to label acidic organelles following the  
585 instructions of the manufacturer. 0.5 µM LysoTracker RedDN99 was added to the tissue culture  
586 medium 30 min before fixing the cells. The residual fluid marker was removed by washing the cells  
587 three times with PBS, followed by fixation.

588         Staining was carried out in 10% horse serum, 0.1% saponin in PBS. Coverslips were washed  
589 twice in PBS containing 0.1% saponin, once in PBS, and incubated for 30 minutes with primary  
590 antibodies. Coverslips were then washed twice in 0.1% saponin in PBS and once in PBS and  
591 incubated for 30 minutes with secondary antibodies. Finally, coverslips were washed twice in 0.1%



592 saponin in PBS, once in PBS and once in H<sub>2</sub>O, mounted on Aqua Poly/Mount (Polysciences).  
593 Immunofluorescence was analysed with a Leica CTR6000 fluorescence microscope. Images were  
594 taken with a Leica DFC350FX monochrome camera. Confocal microscopy was carried out with a  
595 Leica TCS SP5 confocal microscope. Depending of the marker, a KCV was considered positive  
596 when it fulfilled these criteria: (i) the marker was detected throughout the area occupied by the  
597 bacterium; (ii) the marker was detected around/enclosing the bacterium, (iii) the marker was  
598 concentrated in this area, compared to the immediate surroundings. To determine the percentage of  
599 bacteria that colocalized with each marker, all bacteria located inside a minimum of 100 infected  
600 cells were analysed in each experiment. Experiments were carried out by triplicate in three  
601 independent occasions.

602 For extra-/intracellular bacteria differential staining, PFA fixed cells were incubated with  
603 PBS containing 10% horse serum, Hoechst 33342 and rabbit anti-*Klebsiella* for 20 min. Coverslips  
604 were washed three times with PBS and stained as described above with donkey anti-rabbit  
605 conjugated to Rhodamine secondary antibody. Coverslips were washed three times in PBS and once  
606 in distilled water before mounting onto glass slides using Prolong Gold antifade mounting gel  
607 (Invitrogen).

608 For transmission electron microscopy (TEM), cells were seeded in 24-well tissue culture  
609 plates. Infections were carried out as described before, fixed with glutaraldehyde and processed for  
610 TEM as described previously (Kruskal *et al.* 1992).

## 611 **Assessment of intracellular bacteria viability**

### 612 **(i) Fluorescent *in situ* hybridisation**

613 We carried out hybridization of PFA fixed infected cells with fluorescently labelled  
614 oligonucleotides as described before (Morey *et al.* 2011). Alexa488 conjugated DNA probes  
615 EUB338 (5'-GCTGCCTCCCGTAGGAGT-3') and GAM42a (5'-GCCTTCCCACATCGTTT-3')  
616 were designed for specific labelling of rRNA of eubacteria and gamma subclass of Proteobacteria,  
617 respectively (Manz *et al.* 1993). A DNA probe non-EUB338, complementary to EUB338 was used

618 as a negative control. The detectability of bacteria by such oligonucleotide probes is dependent on  
619 the presence of sufficient ribosomes per cell, hence providing qualitative information on the  
620 physiological state of the bacteria on the basis of the number of ribosomes per cell. These probes  
621 were used together to obtain a stronger signal, added to a final concentration of 5 nM each in the  
622 hybridization buffer. The hybridization buffer contained 0.9M NaCl, 20mM Tris-HCl (pH 7.4),  
623 0.01% sodium dodecyl sulfate (SDS) and 35% formamide. Coverslips were first washed with  
624 deionized water. Hybridization was carried out for 1.5 h at 46°C in a humid chamber; followed by a  
625 30 min wash at 48°C. Washing buffer contained 80 mM NaCl, 20 mM Tris-HCl (pH 7.4), 0.01%  
626 sodium dodecyl sulfate (SDS) and 5 mM EDTA (pH 8). After washing, DNA staining for total  
627 bacteria was carried out by incubating the coverslips in PBS containing Hoechst 33342 for 20 min.  
628 Coverslips were then washed three times in PBS and once in distilled water before mounting onto  
629 glass slides using Prolong Gold antifade mounting gel.

## 630 (ii) Two fluorescent markers tagging

631 pJT04mCherry, expressing mCherry constitutively (kindly donated by Miguel Valvano, to  
632 be described elsewhere), and pMMB207gfp3.1 (Pujol *et al.* 2005), expressing *gfpmut3.1* under the  
633 control of an IPTG-inducible promoter, were conjugated into Kp43816R. Control experiments  
634 confirmed that UV-killed *Klebsiella* was always mCherry positive and GFP negative whereas live  
635 *Klebsiella* was mCherry positive and only GFP positive if IPTG was added (1 mM, 1.5 h) to the  
636 medium. Cells were infected with Kp43816R harbouring both plasmids and IPTG was added to the  
637 medium 1.5 h before fixing the cells with PFA. To stain extracellular bacteria, PFA fixed cells were  
638 incubated with PBS containing 10% horse serum, and rabbit anti-*Klebsiella* for 20 min. Coverslips  
639 were washed three times with PBS and stained as described above with goat anti-rabbit antibodies  
640 conjugated to Cascade Blue (C2764, Life Technologies). Immunofluorescence was analysed with a  
641 Leica CTR6000 fluorescence microscope. Images were taken with a Leica DFC350FX  
642 monochrome camera.

## 643 Isolation of *in vivo* infected macrophages

644 Mice were treated in accordance with the Directive of the European Parliament and of the  
645 Council on the protection of animals used for scientific purposes (Directive 2010/63/EU) and in  
646 agreement with the UK Home Office (licence PLZ 2700) and the Bioethical Committee of the  
647 University of the Balearic Islands (authorisation number 1748).

648 Infections were performed as previously described (Insua *et al.* 2013). Briefly, five- to  
649 seven-week-old male C57BL/6 mice (Harlan) were anesthetized by intraperitoneal injection with a  
650 mixture containing ketamine (50 mg/kg) and xylazine (5 mg/kg). Overnight bacterial cultures were  
651 centrifuged (2500 x g, 20 min, 22°C), resuspended in PBS and adjusted to  $5 \times 10^4$  CFU/ml for  
652 determination of bacterial loads. 20 µl of the bacterial suspension were inoculated intranasally in  
653 four 5 µl aliquots. To facilitate consistent inoculations, mice were held vertically during inoculation  
654 and placed on a 45° incline while recovering from anaesthesia. 24 h post infection, mice were  
655 euthanized by cervical dislocation and bronchoalveolar lavage was performed as previously  
656 described (Cai *et al.* 2012). The lavage fluid from four mice was pooled together and spun at 300 x  
657 g for 10 min to pellet alveolar macrophages. Cells were cultured on 12 mm circular coverslips in  
658 24-well tissue culture plates at a concentration of  $0.5 \times 10^6$  cells/well in 1 ml RPMI 1640 tissue  
659 culture medium supplemented with 10% heat-inactivated FCS and 10 mM Hepes and gentamicin  
660 (100 µg/ml). After 2 h of incubation, nonadherent cells were washed off with PBS, and cells were  
661 fixed. Cathepsin D staining was performed as previously described. To label lysosomes using TR-  
662 dextran, after washing off the nonadherent cells, the attached macrophages were pulsed with TR-  
663 dextran (250 µg/ml) for 2 h in RPMI 1640 medium containing gentamicin (100 µg/ml). Cells were  
664 washed three times with PBS, and incubated for 1 h in dye-free medium (chase). After the chase  
665 period, cells were fixed. Immunofluorescence was analysed with a Leica TCS SP5 confocal  
666 microscope.

667 **Neutral red uptake assay for the estimation of cell viability.**

668 Cell viability was determined by assessing the ability of viable cells to incorporate and bind  
669 the supravital dye neutral red in the lysosomes. The protocol described by Repetto and coworkers

670 (Repetto *et al.* 2008) was followed with minor modifications. Macrophages were seeded on 96-well  
671 tissue culture plates at  $5 \times 10^5$  cells/well 18 h before the experiment. Cells were infected to get a  
672 multiplicity of infection of 50:1 in a final volume of 200  $\mu$ l RPMI 1640 tissue culture medium  
673 supplemented with 10% heat-inactivated FCS and 10 mM Hepes. To synchronize infection, plates  
674 were centrifuged at 200 x g during 5 min. Plates were incubated at 37°C in a humidified 5% CO<sub>2</sub>  
675 atmosphere. After 90 min of contact, cells were washed twice with PBS and incubated overnight  
676 with 200  $\mu$ l RPMI 1640 containing 10% FCS, 10 mM Hepes, gentamicin (100  $\mu$ g/ml). Cells were  
677 washed twice with PBS and incubated with 100  $\mu$ l of freshly prepared neutral red medium (final  
678 concentration 40  $\mu$ g/ml neutral red [Sigma] in tissue culture medium) for 2 h. Wells were washed  
679 once with PBS and the remaining biomass-adsorbed neutral red was solubilized with 150  $\mu$ l neutral  
680 red destaining solution (50% ethanol 96%; 49% deionised water, 1% glacial acetic acid). Staining  
681 was then quantified by determining the OD<sub>540</sub> in a 96-well microplate reader, and used to compare  
682 relative neutral red staining of uninfected cells and cells that were lysed completely with 1% Triton  
683 X-100. Experiments were carried out by triplicate in six independent occasions.

#### 684 **Detection of Akt phosphorylation by Western blotting**

685 Macrophages were seeded on 6-well tissue culture plates at  $10^6$  cells/well. Cells were  
686 infected with Kp43816R , washed 3 times with cold PBS, scraped and lysed with 100  $\mu$ l lysis buffer  
687 (1x SDS Sample Buffer, 62.5 mM Tris-HCl pH 6.8, 2% w/v SDS, 10% glycerol, 50 mM DTT,  
688 0.01% w/v bromophenol blue) on ice. Samples were sonicated, boiled at 100°C for 10 min and  
689 cooled on ice before polyacrylamide gel electrophoresis and Western Blotting. Akt phosphorylation  
690 was detected with primary rabbit anti-phospho Ser473 Akt (Cell Signaling Technology) antibody  
691 diluted 1:1,000 and secondary goat anti-rabbit antibody conjugated to horseradish peroxidase  
692 (Thermo Scientific) diluted 1:10,000. Tubulin was detected with primary mouse anti-tubulin  
693 antibody (Sigma) diluted 1:3,000 and secondary goat anti-mouse antibody (Pierce) conjugated to  
694 horseradish peroxidase diluted 1:1,000. To detect tubulin, membranes were reprobed after stripping

695 of previously used antibodies using Western Blot Stripping Buffer (Thermo Scientific). Images  
696 were recorded with a GeneGnome HR imaging system (Syngene).

#### 697 **Apoptosis analysis *in vitro*.**

698 Apoptosis of macrophages was analysed as previously described (Aguilo *et al.* 2013).  
699 Briefly, phosphatidylserine exposure and membrane integrity were analyzed by using Annexin-V  
700 and 7-AAD (BD Biosciences) and FACS according to manufacturer instructions. Cells were  
701 washed with PBS and incubated with APC-conjugated Annexin-V and 7-AAD in Annexin-binding  
702 buffer for 15 min. After that, cells were washed twice with PBS, fixed with 4% PFA during 30 min  
703 and washed again with PBS. Both PBS and PFA contained 2.5 mM CaCl<sub>2</sub>.

#### 704 **Bacterial opsonisation.**

705 Normal human serum (NHS), kindly donated by the Balearics Blood Centre, was obtained  
706 from five different donors (blood type O negative) and kept frozen at -80°C. 35 µl from a  
707 suspension containing approximately 1x10<sup>9</sup> cfu/ml in 10 mM PBS (pH 6.5) were added to 500 µl  
708 RPMI 1640 tissue culture medium supplemented with 10 mM Hepes and 1% NHS. The suspension  
709 was incubated at 37°C shaking (180 rpm) for 45 min. The suspension was used to infect mTHP1  
710 cells as previously described.

#### 711 **Plasmids and transient transfections**

712 For transient transfections with GFP-Rab7 (Addgene plasmid #28047) (Sun *et al.* 2010),  
713 GFP-Rab14 (Kuijl *et al.* 2007), and RILP-C33-EGFP (Cantalupo *et al.* 2001), the Neon transfection  
714 system was used (Life Technologies). 8 x 10<sup>6</sup> cells were transfected (1400 v, 30 ms and 1 pulse)  
715 with 2 µg of plasmid DNA. After, cells were seeded on 12 mm circular coverslips in 24-well tissue  
716 culture plates and 24 h later were infected. In all cases, samples were fixed, stained and analysed by  
717 immunofluorescence microscopy. pcDNA3 and DN-Rab14 (Seto *et al.* 2011) were transfected  
718 using jetPEI-macrophage (Polyplus) following manufacturer's instructions. After 24 h, cells were  
719 washed twice with PBS, infected, and intracellular bacterial load determined as previously  
720 described.

721 **Construction of *cps* reporter strain**

722 DNA fragment containing the promoter region of the Kp43816R capsule operon was  
723 amplified by PCR using *Vent* polymerase (NewEngland Biolabs) and primers K2ProcpsF (5'-  
724 gaattcTGCTGGGACAAATTGCCACC-3') and K2ProcpsR (5'-  
725 AGATGGATGACCCCGCGATC-3'). To construct a green fluorescent protein (GFP) reporter, the  
726 PCR product was EcoRI-digested and cloned into the EcoRI-SmaI digested low-copy-number  
727 vector pPROBE'-gfp[LVA] (Miller *et al.* 2000) to obtain pPROBE'43Procps. The plasmid was  
728 introduced into Kp43816R by electroporation.

729 **Analysis of *cps* expression**

730 The reporter strain was grown at 37°C on an orbital incubator shaker (180 r.p.m.) until  
731 OD<sub>540</sub> 1.2. The cultures were harvested (2500 x g, 20 min, 24°C) and resuspended to an OD<sub>540</sub> of  
732 0.6 in PBS. 0.8-ml aliquot of this suspension was transferred to 1-cm fluorimetric cuvette and  
733 fluorescence was measured with a spectrofluorophotometer (Perkin Elmer LS55) set as follows:  
734 excitation, 485 nm; emission, 528 nm; slit width 5 nm; integration time 5 seconds. Results were  
735 expressed as relative fluorescence units (RFU). All measurements were carried out in quintuplicate  
736 on at least three separate occasions.

737 To obtain RNA, bacteria were grown at 37°C in 5 ml of medium on an orbital incubator  
738 shaker (180 r.p.m.) until an OD<sub>600</sub> of 0.3. 3 ml of RNA later solution were added to the culture and  
739 the mixture was incubated for 20 min to prevent RNA degradation. Total RNA was extracted using  
740 Trizol as recommended by the manufacturer (Life Technology). The purification included a  
741 DNAase treatment step. cDNA was obtained by retrotranscription of 1 µg of total RNA using a  
742 commercial M-MLV Reverse Transcriptase (Sigma), and random primers mixture (Invitrogen). 20  
743 ng of cDNA were used as a template in a 10-µl reaction. RT-PCR analyses were performed with a  
744 Mx3005P qPCR System (Agilent Technologies) and using a KapaSYBR Fast qPCR Kit as  
745 recommended by the manufacturer (Kapa biosystems). The thermocycling protocol was as follows;  
746 95°C for 3 min for hot-start polymerase activation, followed by 40 cycles of 95°C for 10 s, and

747 56°C for 20 s. SYBR green dye fluorescence was measured at 521 nm. cDNAs were obtained from  
748 two independent extractions of mRNA and each one amplified by RT-qPCR in two independent  
749 occasions. Relative quantities of *wzi*, *orf7* and *gnd* mRNAs were obtained using the comparative  
750 threshold cycle ( $\Delta\Delta CT$ ) method by normalizing to *rpoD* gene. Primers used were: Kpn\_RpoD\_F1  
751 (5'-CCGGAAGACAAAATCCGTAA-3') and Kpn\_RpoD\_R1 (5'-  
752 CGGGTAACGTCGAACTGTTT-3'); Kp43/52\_wzi\_F2 (5'-TCGACCGCAATCATTTCAGCA-3')  
753 and Kp43/52\_wzi\_R2 (5'-CATCCTTACCCCAGCCGTG-3'); Kp43/52\_orf7\_F1 (5'-  
754 ATCAAGATTGCCGACGTTTCT-3') and Kp43/52\_orf7\_R1 (5'-  
755 GCCTCTACCGCAACTAATCCA-3'); Kp43/52\_gnd\_F1 (5'-GGATC CGGCGAACCTCTTT-3')  
756 and Kp43/52\_gnd\_R1 (5'-GCCCTGAGCATAGGAAACGA-3').

757 For analysis of *cps* expression from intracellular bacteria, macrophages were seeded in 6-  
758 well plates and infected with Kp43816R containing pPROBE'43Procps or pPROBE'-gfp[LVA]  
759 control vector at a MOI of 150:1. After 40 min, cells were washed twice with PBS and incubated  
760 with 500  $\mu$ l RPMI 1640 containing 10% FCS, 10 mM Hepes, gentamicin (300  $\mu$ g/ml) and  
761 polymyxin B (15  $\mu$ g/ml) to eliminate extracellular bacteria. At the indicated time points, cells were  
762 lysed with 900  $\mu$ l 0.5 % saponin in PBS. The samples from two wells were combined and serial  
763 dilutions were plated on LB to quantify the number of intracellular bacteria. Control experiments  
764 showed that there were no differences in the number of intracellular bacteria recovered over time  
765 from cells infected with bacteria containing pPROBE'-gfp[LVA] derivatives or no plasmid (data  
766 not shown). By replica plating on plates containing kanamycin, it was determined that 85-100% of  
767 the bacteria contained the reporter plasmid at any time point analysed. The rest of the lysate was  
768 centrifuged (13 000 rpm, 1 min, room temperature) and resuspended in 1 ml 1 % BSA in PBS for  
769 staining. Bacteria were stained with rabbit anti-*Klebsiella* serum diluted 1:5000 for 20 min, washed  
770 twice with PBS, and incubated for 20 min with a 1:200 dilution of Rhodamine-conjugated donkey  
771 anti-rabbit secondary antibody. Flow cytometry analyses were performed using a Cultek Epics XL  
772 flow cytometer. Samples were gated for bacteria-like particles by using the rhodamine fluorescence

773 of the anti-*Klebsiella* labelling to identify bacterial cells and to exclude mammalian cell debris and  
774 background noise. Lysed and stained uninfected macrophages were not rhodamine positive,  
775 indicating that there was no cross-reactivity of the primary or secondary antibodies with MH-S  
776 cells. Fluorescence compensation settings were determined in parallel under identical conditions by  
777 using the constitutively GFP-expressing Kp43816R strain or the non-expressing strain, with and  
778 without anti-*Klebsiella* antibody labelling. Approximately 10,000 events identified as *Klebsiella*  
779 cells were collected per sample. A histogram of GFP fluorescence for the negative-control sample  
780 (bacteria containing pPROBE'-gfp[LVA] ) was created, and the area of the histogram containing  
781 the bacterial population was considered to be negative for GFP fluorescence. All experiments were  
782 done with triplicate samples on at least three independent occasions.

### 783 **Statistical analysis.**

784 Statistical analyses were performed using the one-tailed *t* test or, when the requirements  
785 were not met, by the Mann-Whitney U test.  $P < 0.05$  was considered statistically significant. The  
786 analyses were performed using Prism4 for PC (GraphPad Software).

787

### 788 **ACKNOWLEDGEMENTS**

789 We are grateful to members of Bengoechea lab for helpful discussions. We are indebted to Miguel  
790 Valvano, Sergio Grinstein, Jacques Neefjes, Jim Bliska and Yukio Koide for sending us plasmids  
791 and helpful discussions. M.I.M.-L. was financially supported by the Instituto de Salud Carlos III  
792 (grant CM09/000123). Part of this work was supported by grant PS09-00130 from Instituto de  
793 Salud Carlos III to J.G., and by grants from Biomedicine Program (SAF2009-07885 and SAF2012-  
794 39841) from Ministerio de Economía y Competitividad (Spain), Govern Illes Balears (Competitive  
795 group Ref: 46/2011); and Queen's University Belfast start-up funds to J.A.B. This research was also  
796 supported by a Marie Curie FP7 Integration Grant (U-KARE; PCIG13-GA-2013-618162) to J.A.B.  
797 within the 7th European Union Framework Programme. CIBERES is an initiative from Instituto de  
798 Salud Carlos III.



800 **REFERENCES**

- 801 Aderem, A., and Underhill, D.M. (1999) Mechanisms of phagocytosis in macrophages. *Annu Rev*  
802 *Immunol* 17: 593-623.
- 803 Aguilo, J.I., Alonso, H., Uranga, S., Marinova, D., Arbues, A., de Martino, A., *et al* (2013) ESX-1-  
804 induced apoptosis is involved in cell-to-cell spread of *Mycobacterium tuberculosis*. *Cell Microbiol*  
805 15: 1994-2005.
- 806 Alvarez, D., Merino, S., Tomas, J.M., Benedi, V.J., and Alberti, S. (2000) Capsular polysaccharide  
807 is a major complement resistance factor in lipopolysaccharide O side chain-deficient *Klebsiella*  
808 *pneumoniae* clinical isolates. *Infect Immun* 68: 953-955.
- 809 Arakawa, Y., Wacharotayankun, R., Nagatsuka, T., Ito, H., Kato, N., and Ohta, M. (1995) Genomic  
810 organization of the *Klebsiella pneumoniae cps* region responsible for serotype K2 capsular  
811 polysaccharide synthesis in the virulent strain Chedid. *J Bacteriol* 177: 1788-1796.
- 812 Bakker-Woudenberg, I.A., van den Berg J.C., Vree T.B., Baars A.M., and Michel M.F. (1985)  
813 Relevance of serum protein binding of cefoxitin and cefazolin to their activities against *Klebsiella*  
814 *pneumoniae* pneumonia in rats. *Antimicrob Agents Chemother* 28:654-659.
- 815 Broug-Holub, E., Toews, G.B., van Iwaarden, J.F., Strieter, R.M., Kunkel, S.L., Paine, R., 3rd, *et al*  
816 (1997) Alveolar macrophages are required for protective pulmonary defenses in murine *Klebsiella*  
817 pneumonia: elimination of alveolar macrophages increases neutrophil recruitment but decreases  
818 bacterial clearance and survival. *Infect Immun* 65: 1139-1146.
- 819 Cai, S., Batra, S., Wakamatsu, N., Pacher, P., and Jeyaseelan, S. (2012) NLRC4 inflammasome-  
820 mediated production of IL-1 $\beta$  modulates mucosal immunity in the lung against gram-negative  
821 bacterial infection. *J Immunol* 188: 5623-5635.
- 822 Campos, M.A., Vargas, M.A., Regueiro, V., Llompарт, C.M., Alberti, S., and Bengoechea, J.A.  
823 (2004) Capsule polysaccharide mediates bacterial resistance to antimicrobial peptides. *Infect Immun*  
824 72: 7107-7114.
- 825 Camprubi, S., Merino, S., Benedi, V.J., and Tomas, J.M. (1993) The role of the O-antigen  
826 lipopolysaccharide and capsule on an experimental *Klebsiella pneumoniae* infection of the rat  
827 urinary tract. *FEMS Microbiol Lett* 111: 9-13.
- 828 Cano, V., Moranta, D., Llobet-Brossa, E., Bengoechea, J.A., and Garmendia, J. (2009) *Klebsiella*  
829 *pneumoniae* triggers a cytotoxic effect on airway epithelial cells. *BMC Microbiol* 9: 156-2180-9-  
830 156.
- 831 Cantalupo, G., Alifano, P., Roberti, V., Bruni, C.B., and Bucci, C. (2001) Rab-interacting  
832 lysosomal protein (RILP): the Rab7 effector required for transport to lysosomes. *EMBO J* 20: 683-  
833 693.
- 834 Cheung, D.O., Halsey, K., and Speert, D.P. (2000) Role of pulmonary alveolar macrophages in  
835 defense of the lung against *Pseudomonas aeruginosa*. *Infect Immun* 68: 4585-4592.
- 836 Chiu, H.C., Soni, S., Kulp, S.K., Curry, H., Wang, D., Gunn, J.S., *et al* (2009) Eradication of  
837 intracellular *Francisella tularensis* in THP-1 human macrophages with a novel autophagy inducing  
838 agent. *J Biomed Sci* 16: 110-0127-16-110.
- 839 Christensen, H., Hansen, M., and Sorensen, J. (1999) Counting and size classification of active soil  
840 bacteria by fluorescence in situ hybridization with an rRNA oligonucleotide probe. *Appl Environ*  
841 *Microbiol* 65: 1753-1761.

842 Cortes, G., Alvarez, D., Saus, C., and Alberti, S. (2002a) Role of lung epithelial cells in defense  
843 against *Klebsiella pneumoniae* pneumonia. *Infect Immun* 70: 1075-1080.

844 Cortes, G., Borrell, N., de Astorza, B., Gomez, C., Sauleda, J., and Alberti, S. (2002b) Molecular  
845 analysis of the contribution of the capsular polysaccharide and the lipopolysaccharide O side chain  
846 to the virulence of *Klebsiella pneumoniae* in a murine model of pneumonia. *Infect Immun* 70: 2583-  
847 2590.

848 Datsenko, K.A., and Wanner, B.L. (2000) One-step inactivation of chromosomal genes in  
849 *Escherichia coli* K-12 using PCR products. *Proc Natl Acad Sci U S A* 97: 6640-6645.

850 de Astorza, B., Cortes, G., Crespi, C., Saus, C., Rojo, J.M., and Alberti, S. (2004) C3 promotes  
851 clearance of *Klebsiella pneumoniae* by A549 epithelial cells. *Infect Immun* 72: 1767-1774.

852 Derbise, A., Lesic, B., Dacheux, D., Ghigo, J.M., and Carniel, E. (2003) A rapid and simple method  
853 for inactivating chromosomal genes in *Yersinia*. *FEMS Immunol Med Microbiol* 38: 113-116.

854 Drecktrah, D., Knodler, L.A., Ireland, R., and Steele-Mortimer, O. (2006) The mechanism of  
855 *Salmonella* entry determines the vacuolar environment and intracellular gene expression. *Traffic* 7:  
856 39-51.

857 Drevets, D.A., Leenen, P.J., and Campbell, P.A. (1993) Complement receptor type 3  
858 (CD11b/CD18) involvement is essential for killing of *Listeria monocytogenes* by mouse  
859 macrophages. *J Immunol* 151: 5431-5439.

860 Eissenberg, L.G., Schlesinger, P.H., and Goldman, W.E. (1988) Phagosome-lysosome fusion in  
861 P388D1 macrophages infected with *Histoplasma capsulatum*. *J Leukoc Biol* 43: 483-491.

862 Fevre, C., Almeida, A.S., Taront, S., Pedron, T., Huerre, M., Prevost, M.C., *et al* (2013) A novel  
863 murine model of rhinoscleroma identifies Mikulicz cells, the disease signature, as IL-10 dependent  
864 derivatives of inflammatory monocytes. *EMBO Mol Med* 5: 516-530.

865 Fink, S.L., and Cookson, B.T. (2007) Pyroptosis and host cell death responses during *Salmonella*  
866 infection. *Cell Microbiol* 9: 2562-2570.

867 Finlay, B.B., and McFadden, G. (2006) Anti-immunology: evasion of the host immune system by  
868 bacterial and viral pathogens. *Cell* 124: 767-782.

869

870 Flannagan, R.S., Cosio, G., and Grinstein, S. (2009) Antimicrobial mechanisms of phagocytes and  
871 bacterial evasion strategies. *Nat Rev Microbiol* 7: 355-366.

872 Flannagan, R.S., Jaumouille, V., and Grinstein, S. (2012) The cell biology of phagocytosis. *Annu*  
873 *Rev Pathol* 7: 61-98.

874 Fortier, A.H., Leiby, D.A., Narayanan, R.B., Asafodjei, E., Crawford, R.M., Nacy, C.A., *et al*  
875 (1995) Growth of *Francisella tularensis* LVS in macrophages: the acidic intracellular compartment  
876 provides essential iron required for growth. *Infect Immun* 63: 1478-1483.

877 Frank, C.G., Reguerio, V., Rother, M., Moranta, D., Maeurer, A.P., Garmendia, J., *et al* (2013)  
878 *Klebsiella pneumoniae* targets an EGF receptor-dependent pathway to subvert inflammation. *Cell*  
879 *Microbiol* 15: 1212-1233.

880 Garcia-del Portillo, F., Foster, J.W., Maguire, M.E., and Finlay, B.B. (1992) Characterization of the  
881 micro-environment of *Salmonella typhimurium*-containing vacuoles within MDCK epithelial cells.  
882 *Mol Microbiol* 6: 3289-3297.

883 Geier, H., and Celli, J. (2011) Phagocytic receptors dictate phagosomal escape and intracellular  
884 proliferation of *Francisella tularensis*. *Infect Immun* 79: 2204-2214.

885 Ghigo, E., Capo, C., Aurouze, M., Tung, C.H., Gorvel, J.P., Raoult, D., *et al* (2002) Survival of  
886 *Tropheryma whipplei*, the agent of Whipple's disease, requires phagosome acidification. *Infect*  
887 *Immun* 70: 1501-1506.

888 Gordon, S.B., Irving, G.R., Lawson, R.A., Lee, M.E., and Read, R.C. (2000) Intracellular  
889 trafficking and killing of *Streptococcus pneumoniae* by human alveolar macrophages are influenced  
890 by opsonins. *Infect Immun* 68: 2286-2293.

891 Greco, E., Quintiliani, G., Santucci, M.B., Serafino, A., Ciccaglione, A.R., Marcantonio, C., *et al*  
892 (2012) Janus-faced liposomes enhance antimicrobial innate immune response in *Mycobacterium*  
893 *tuberculosis* infection. *Proc Natl Acad Sci U S A* 109: E1360-8.

894 Greenberger, M.J., Kunkel, S.L., Strieter, R.M., Lukacs, N.W., Bramson, J., Gauldie, J., *et al*  
895 (1996a) IL-12 gene therapy protects mice in lethal *Klebsiella* pneumonia. *J Immunol* 157: 3006-  
896 3012.

897  
898 Greenberger, M.J., Strieter, R.M., Kunkel, S.L., Danforth, J.M., Laichalk, L.L., McGillicuddy,  
899 D.C., *et al* (1996b) Neutralization of macrophage inflammatory protein-2 attenuates neutrophil  
900 recruitment and bacterial clearance in murine *Klebsiella* pneumonia. *J Infect Dis* 173: 159-165.  
901

902 Happel, K.I., Dubin, P.J., Zheng, M., Ghilardi, N., Lockhart, C., Quinton, L.J., *et al* (2005)  
903 Divergent roles of IL-23 and IL-12 in host defense against *Klebsiella pneumoniae*. *J Exp Med* 202:  
904 761-769.

905  
906 Happel, K.I., Zheng, M., Young, E., Quinton, L.J., Lockhart, E., Ramsay, A.J., *et al* (2003) Cutting  
907 edge: roles of Toll-like receptor 4 and IL-23 in IL-17 expression in response to *Klebsiella*  
908 *pneumoniae* infection. *J Immunol* 170: 4432-4436.

909  
910 Hilbi, H., Moss, J.E., Hersh, D., Chen, Y., Arondel, J., Banerjee, S., *et al* (1998) *Shigella*-induced  
911 apoptosis is dependent on caspase-1 which binds to IpaB. *J Biol Chem* 273: 32895-32900.

912 Hmama, Z., Sendide, K., Talal, A., Garcia, R., Dobos, K., and Reiner, N.E. (2004) Quantitative  
913 analysis of phagolysosome fusion in intact cells: inhibition by mycobacterial lipoarabinomannan  
914 and rescue by an 1alpha,25-dihydroxyvitamin D3-phosphoinositide 3-kinase pathway. *J Cell Sci*  
915 117: 2131-2140.

916 Hoogendijk, A.J., Diks, S.H., Peppelenbosch, M.P., Van Der Poll, T., and Wieland, C.W. (2011)  
917 Kinase activity profiling of gram-negative pneumonia. *Mol Med* 17: 741-747.

918 Howe, D., and Mallavia, L.P. (2000) *Coxiella burnetii* exhibits morphological change and delays  
919 phagolysosomal fusion after internalization by J774A.1 cells. *Infect Immun* 68: 3815-3821.

920 Insua, J.L., Llobet, E., Moranta, D., Perez-Gutierrez, C., Tomas, A., Garmendia, J., *et al* (2013)  
921 Modelling *Klebsiella pneumoniae* pathogenesis by infecting the wax moth *Galleria mellonella*.  
922 *Infect Immun.* 81: 3552-3565.

923 Jordens, I., Fernandez-Borja, M., Marsman, M., Dusseljee, S., Janssen, L., Calafat, J., *et al* (2001)  
924 The Rab7 effector protein RILP controls lysosomal transport by inducing the recruitment of dynein-  
925 dynactin motors. *Curr Biol* 11: 1680-1685.

926 Krachler, A.M., Woolery, A.R., and Orth, K. (2011) Manipulation of kinase signaling by bacterial  
927 pathogens. *J Cell Biol* 195: 1083-1092.

928 Kruskal, B.A., Sastry, K., Warner, A.B., Mathieu, C.E., and Ezekowitz, R.A. (1992) Phagocytic  
929 chimeric receptors require both transmembrane and cytoplasmic domains from the mannose  
930 receptor. *J Exp Med* 176: 1673-1680.

931 Kuijl, C., Savage, N.D., Marsman, M., Tuin, A.W., Janssen, L., Egan, D.A., *et al* (2007)  
932 Intracellular bacterial growth is controlled by a kinase network around PKB/AKT1. *Nature* 450:  
933 725-730.

934 Kyei, G.B., Vergne, I., Chua, J., Roberts, E., Harris, J., Junutula, J.R., *et al* (2006) Rab14 is critical  
935 for maintenance of *Mycobacterium tuberculosis* phagosome maturation arrest. *EMBO J* 25: 5250-  
936 5259.

937 Lamothe, J., Huynh, K.K., Grinstein, S., and Valvano, M.A. (2007) Intracellular survival of  
938 *Burkholderia cenocepacia* in macrophages is associated with a delay in the maturation of bacteria-  
939 containing vacuoles. *Cell Microbiol* 9: 40-53.

940 Lawlor, M.S., Handley, S.A., and Miller, V.L. (2006) Comparison of the host responses to wild-  
941 type and *cpsB* mutant *Klebsiella pneumoniae* infections. *Infect Immun* 74: 5402-5407.

942 Lawlor, M.S., Hsu, J., Rick, P.D., and Miller, V.L. (2005) Identification of *Klebsiella pneumoniae*  
943 virulence determinants using an intranasal infection model. *Mol Microbiol* 58: 1054-1073.

944 Manz, W., Szewzyk, U., Ericsson, P., Amann, R., Schleifer, K.H., and Stenstrom, T.A. (1993) In  
945 situ identification of bacteria in drinking water and adjoining biofilms by hybridization with 16S  
946 and 23S rRNA-directed fluorescent oligonucleotide probes. *Appl Environ Microbiol* 59: 2293-2298.

947 March, C., Cano, V., Moranta, D., Llobet, E., Perez-Gutierrez, C., Tomas, J.M., *et al* (2013) Role of  
948 bacterial surface structures on the interaction of *Klebsiella pneumoniae* with phagocytes. *PLoS One*  
949 8: e56847.

950 Miller, W.G., Leveau, J.H., and Lindow, S.E. (2000) Improved *gfp* and *inaZ* broad-host-range  
951 promoter-probe vectors. *Mol Plant Microbe Interact* 13: 1243-1250.

952 Moranta, D., Regueiro, V., March, C., Llobet, E., Margareto, J., Larrarte, E., *et al* (2010) *Klebsiella*  
953 *pneumoniae* capsule polysaccharide impedes the expression of beta-defensins by airway epithelial  
954 cells. *Infect Immun* 78: 1135-1146.

955 Morey, P., Cano, V., Marti-Llitas, P., Lopez-Gomez, A., Regueiro, V., Saus, C., *et al* (2011)  
956 Evidence for a non-replicative intracellular stage of nontypable *Haemophilus influenzae* in  
957 epithelial cells. *Microbiology* 157: 234-250.

958 Munoz-Price, L.S., Poirel, L., Bonomo, R.A., Schwaber, M.J., Daikos, G.L., Cormican, M., *et al*  
959 (2013) Clinical epidemiology of the global expansion of *Klebsiella pneumoniae* carbapenemases.  
960 *Lancet Infect Dis* 13: 785-796.

961 Navarre, W.W., and Zychlinsky, A. (2000) Pathogen-induced apoptosis of macrophages: a common  
962 end for different pathogenic strategies. *Cell Microbiol* 2: 265-273.

963 Oelschlaeger, T.A., and Tall, B.D. (1997) Invasion of cultured human epithelial cells by *Klebsiella*  
964 *pneumoniae* isolated from the urinary tract. *Infect Immun* 65: 2950-2958.

965 Porte, F., Liautard, J.P., and Kohler, S. (1999) Early acidification of phagosomes containing  
966 *Brucella suis* is essential for intracellular survival in murine macrophages. *Infect Immun* 67: 4041-  
967 4047.

968 Pujol, C., Grabenstein, J.P., Perry, R.D., and Bliska, J.B. (2005) Replication of *Yersinia pestis* in  
969 interferon gamma-activated macrophages requires *ripA*, a gene encoded in the pigmentation locus.  
970 *Proc Natl Acad Sci U S A* 102: 12909-12914.

971

972 Regueiro, V., Campos, M.A., Pons, J., Alberti, S., and Bengoechea, J.A. (2006) The uptake of a  
973 *Klebsiella pneumoniae* capsule polysaccharide mutant triggers an inflammatory response by human  
974 airway epithelial cells. *Microbiology* 152: 555-566.

975 Repetto, G., del Peso, A., and Zurita, J.L. (2008) Neutral red uptake assay for the estimation of cell  
976 viability/cytotoxicity. *Nat Protoc* 3: 1125-1131.

977 Rink, J., Ghigo, E., Kalaidzidis, Y., and Zerial, M. (2005) Rab conversion as a mechanism of  
978 progression from early to late endosomes. *Cell* 122: 735-749.

979 Sahly, H., and Podschun, R. (1997) Clinical, bacteriological, and serological aspects of *Klebsiella*  
980 infections and their spondylarthropathic sequelae. *Clin Diagn Lab Immunol* 4: 393-399.

981 Sarantis, H., and Grinstein, S. (2012) Subversion of phagocytosis for pathogen survival. *Cell Host*  
982 *Microbe* 12: 419-431.

983 Seto, S., Tsujimura, K., and Koide, Y. (2011) Rab GTPases regulating phagosome maturation are  
984 differentially recruited to mycobacterial phagosomes. *Traffic* 12: 407-420.

985 Smith, A.C., Heo, W.D., Braun, V., Jiang, X., Macrae, C., Casanova, J.E., *et al* (2007) A network  
986 of Rab GTPases controls phagosome maturation and is modulated by *Salmonella enterica* serovar  
987 Typhimurium. *J Cell Biol* 176: 263-268.

988 Sun, Q., Westphal, W., Wong, K.N., Tan, I., and Zhong, Q. (2010) Rubicon controls endosome  
989 maturation as a Rab7 effector. *Proc Natl Acad Sci U S A* 107: 19338-19343.

990

991 Thi, E.P., and Reiner, N.E. (2012) Phosphatidylinositol 3-kinases and their roles in phagosome  
992 maturation. *J Leukoc Biol* 92: 553-566.

993 Trombetta, E.S., and Mellman, I. (2005) Cell biology of antigen processing in vitro and in vivo.  
994 *Annu Rev Immunol* 23: 975-1028.

995 Vieira, O.V., Botelho, R.J., and Grinstein, S. (2002) Phagosome maturation: aging gracefully.  
996 *Biochem J* 366: 689-704.

997 Vieira, O.V., Botelho, R.J., Rameh, L., Brachmann, S.M., Matsuo, T., Davidson, H.W., *et al* (2001)  
998 Distinct roles of class I and class III phosphatidylinositol 3-kinases in phagosome formation and  
999 maturation. *J Cell Biol* 155: 19-25.

1000 von Bargen, K., Gorvel, J.P., and Salcedo, S.P. (2012) Internal affairs: investigating the *Brucella*  
1001 intracellular lifestyle. *FEMS Microbiol Rev* 36: 533-562.

1002 Willingham, S.B., Allen, I.C., Bergstralh, D.T., Brickey, W.J., Huang, M.T., Taxman, D.J., *et al*  
1003 (2009) NLRP3 (NALP3, Cryopyrin) facilitates in vivo caspase-1 activation, necrosis, and HMGB1  
1004 release via inflammasome-dependent and -independent pathways. *J Immunol* 183: 2008-2015.

1005 Willingham, S.B., Bergstralh, D.T., O'Connor, W., Morrison, A.C., Taxman, D.J., Duncan, J.A., *et*  
1006 *al* (2007) Microbial pathogen-induced necrotic cell death mediated by the inflammasome  
1007 components CIAS1/cryopyrin/NLRP3 and ASC. *Cell Host Microbe* 2: 147-159.

1008 Wu, J., Kobayashi, M., Sousa, E.A., Liu, W., Cai, J., Goldman, S.J., *et al* (2005) Differential  
1009 proteomic analysis of bronchoalveolar lavage fluid in asthmatics following segmental antigen  
1010 challenge. *Mol Cell Proteomics* 4: 1251-1264.

1011 Yu, X.J., McGourty, K., Liu, M., Unsworth, K.E., and Holden, D.W. (2010) pH sensing by  
1012 intracellular *Salmonella* induces effector translocation. *Science* 328: 1040-1043.

1013 Zimmerli, S., Edwards, S., and Ernst, J.D. (1996) Selective receptor blockade during phagocytosis  
1014 does not alter the survival and growth of *Mycobacterium tuberculosis* in human macrophages. *Am J*  
1015 *Respir Cell Mol Biol* 15: 760-770.

1016

1017

1018

## 1019 **FIGURE LEGENDS**

### 1020 **FIGURE 1. Phagocytosis of *K. pneumoniae* by macrophages.**

1021 (A) Immunofluorescence confocal microscopy showing the lack of colocalisation between *K.*  
1022 *pneumoniae* and the lysosome marker cathepsin D or TR-dextran (pulse-chase experiment  
1023 described in Experimental procedures) in macrophages isolated from the BALF of infected mice  
1024 with Kp43816R harbouring pFPV25.1Cm. Methanol fixation was used for cathepsin D staining. (B)  
1025 Involvement of PI3K, cytoskeleton and lipid rafts on Kp43816R phagocytosis by MH-S cells. (C)  
1026 Immunoblot analysis of Akt phosphorylation (P-Akt) in lysates of MH-S cells infected with live or  
1027 UV-killed Kp43816R for the indicated times (in minutes). Membranes were probed for tubulin as a  
1028 loading control. Images are representative of three independent experiments. (D) Immunoblot  
1029 analysis of Akt phosphorylation (P-Akt) in lysates of PI3K inhibitor (LY294002) or DMSO  
1030 (vehicle solution)-treated MH-S cells infected with Kp43816R for 20 min. Membranes were probed  
1031 for tubulin as a loading control. Images are representative of three independent experiments.

### 1032 **FIGURE 2. Dynamics of *K. pneumoniae* survival in MH-S cells.**

1033 (A) MH-S cells were infected with Kp43816R for 30 min (MOI 50:1). Wells were washed and  
1034 incubated with medium containing gentamicin (300 µg/ml) and polymyxin B (15 µg/ml) for 90 min  
1035 to eliminate extracellular bacteria, and then with medium containing gentamicin 100 µg/ml for up to  
1036 7.5 h. Intracellular bacteria were quantified by lysis, serial dilution and viable counting on LB agar  
1037 plates. (B) MH-S cells were infected with Kp43816R harboring pFPV25.1Cm and the percentage of  
1038 macrophages containing intracellular bacteria (determined by extra-/intracellular differential  
1039 staining) assessed over time. Extracellular bacteria were stained using rabbit anti-*Klebsiella*  
1040 antibodies detected using donkey anti-rabbit conjugated to Rhodamine secondary antibodies. (C)  
1041 Percentage of infected macrophages containing 1-2; 3-5, or more than 5 intracellular bacteria  
1042 (determined by extra-/intracellular differential staining) over time. (D) MH-S cells were infected  
1043 with Kp43816R harbouring pJT04mCherry, expressing mCherry constitutively, and  
1044 pMMB207gfp3.1, expressing *gfpmut3.1* under the control of an IPTG-inducible promoter. IPTG (1

1045 mM) was added 1.5 h before fixation. Images were taken 3.5 h post infection. Images are  
1046 representative of duplicate coverslips in three independent experiments. (E) Percentage of  
1047 intracellular bacteria (determined by extra-/intracellular differential staining; *Klebsiella* antibodies  
1048 were detected using goat anti-rabbit conjugated to Cascade blue antibodies) mCherry-GFP positive  
1049 over time. In panel A, data, shown as  $\text{Log}_{10}\text{CFU/well}$ , are the average of three independent  
1050 experiments. In panel B, at least 500 cells belonging to three independent experiments were counted  
1051 per time point whereas in panels C and E, at least 300 infected cells from three independent  
1052 experiments were counted per time point.

1053 **FIGURE 3. Apoptosis of MH-S cells.**

1054 (A) MH-S cells were mock-treated or infected with Kp43816R harboring pFPV25.1Cm. 6 h post  
1055 infection, cells were stained with Annexin V and 7-AAD and analysed by flow cytometry. A  
1056 representative experiment of three is shown. (B) Data from three independent experiments are  
1057 represented as mean  $\pm$  SD.

1058 **FIGURE 4. Phagosome maturation during *K. pneumoniae* infection of MH-S cells.**

1059 (A) Upper and middle rows show the colocalization of Kp43816R harboring pFPV25.1Cm and  
1060 EEA1 (images were taken 30 min post infection) and Lamp1 (images were taken 4 h post infection)  
1061 using goat anti-EEA1 and donkey anti-goat conjugated to Rhodamine, and rat anti-Lamp-1 and  
1062 donkey anti-rat conjugated to Rhodamine antibodies, respectively. Images are representative of  
1063 triplicate coverslips in three independent experiments. (B) Panels show the colocalization of  
1064 Kp431816R and Lamp1 and EGFP-Rab7 or RILP-C33-EGFP (images were taken 3.5 h post  
1065 infection). Bacteria were stained using rabbit anti-*Klebsiella* and goat anti-rabbit conjugated to  
1066 Cascade blue antibodies. Images are representative of triplicate coverslips in three independent  
1067 experiments. (C) Percentage of Kp43816R colocalization with EEA1, Lamp1, and EGFP-Rab7 and  
1068 RILP-C33-EGFP over a time course. Cells were infected, coverslips were fixed and stained at the  
1069 indicated times. Values are given as mean percentage of Kp43816R colocalizing with the marker  $\pm$

1070 SE. At least 300 infected cells belonging to three independent experiments were counted per time  
1071 point.

1072 **FIGURE 5. Colocalization of *K. pneumoniae* with phagolysosomal markers.**

1073 (A) Upper row shows the colocalization of Kp43816R harboring pFPV25.1Cm and the dye  
1074 LysoTracker at 4 h post infection. Middle row shows the colocalization of Kp43816R harboring  
1075 pFPV25.1Cm and cathepsin D at 2 h post infection. Cathepsin D was stained using goat anti-human  
1076 cathepsin D (G19) and donkey anti-goat conjugated to Rhodamine antibodies. Lower row displays  
1077 the colocalization of Kp43816R harboring pFPV25.1Cm and TR-dextran at 2 h post infection.  
1078 Images are representative of three independent experiments. (B) Percentage of Kp43816R  
1079 colocalization with LysoTracker, cathepsin D and TR-dextran over a time course. Cells were  
1080 infected, coverslips were fixed and stained at the indicated times. Values are given as mean  
1081 percentage of Kp43816R colocalizing with the marker  $\pm$  SE. At least 300 infected cells belonging  
1082 to three independent experiments were counted per time point.

1083 **FIGURE 6. Effect of vacuolar acidification on *K. pneumoniae* survival.**

1084 (A) Microscopy analysis showing that bafilomycin A<sub>1</sub> (100 nM) treatment abrogates LysoTracker  
1085 staining of the KCV (images were taken at 4 h post infection). MH-S cells were infected with  
1086 Kp43816R harboring pFPV25.1Cm. Images are representative of triplicate coverslips in two  
1087 independent experiments. (B) Experimental outline to investigate the effect of vacuolar acidification  
1088 on the intracellular survival of Kp43816R. (C) Intracellular bacteria in MH-S cells, treated (white  
1089 symbols) or not (black symbols) with bafilomycin A<sub>1</sub>, were quantified by lysis, serial dilution and  
1090 viable counting on LB agar plates. Data, shown as CFU/well, are the average of three independent  
1091 experiments. Significance testing performed by Log Rank test. \*,  $P < 0.05$ .

1092 **FIGURE 7. PI3K-AKT and Rab14 aid intracellular survival of *K. pneumoniae*.**

1093 (A) Quantification of intracellular bacteria in MH-S cells infected with Kp43816R which were  
1094 mock-treated (black bar) or treated with LY294002 hydrochloride (75  $\mu$ M) or with AKT X (10  
1095  $\mu$ M). Treatments were added after the time of contact and kept until cells were lysed for bacterial

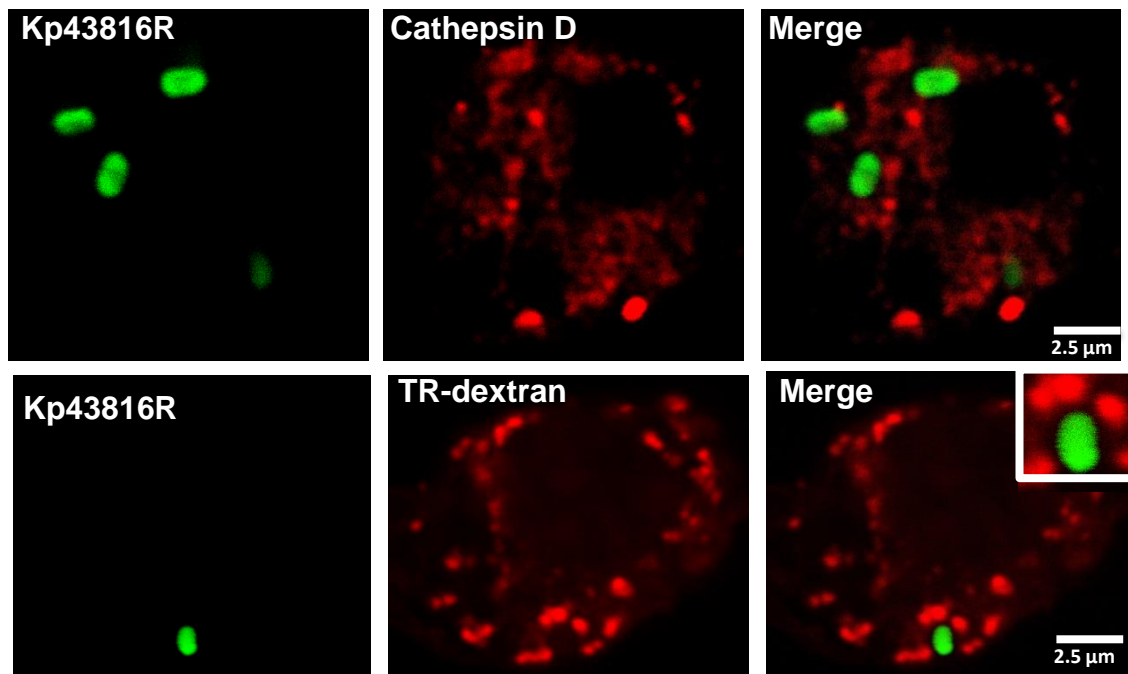
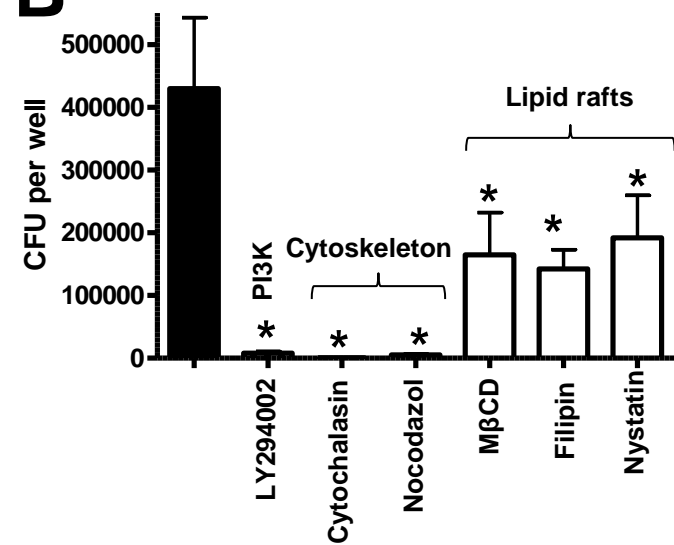
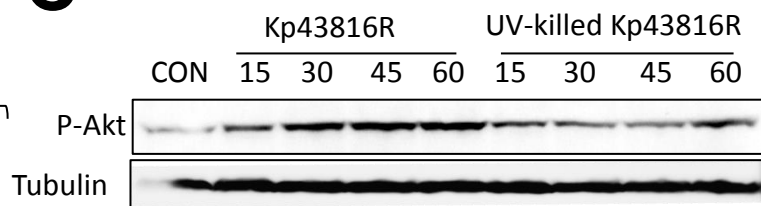
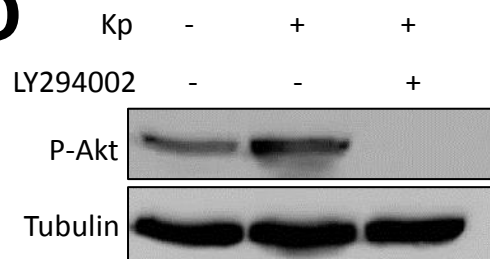


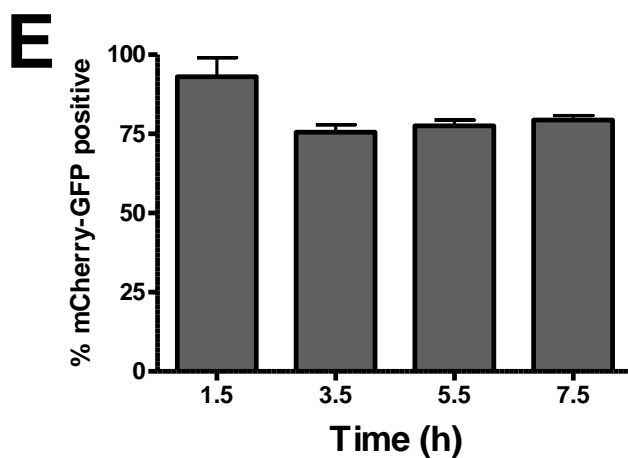
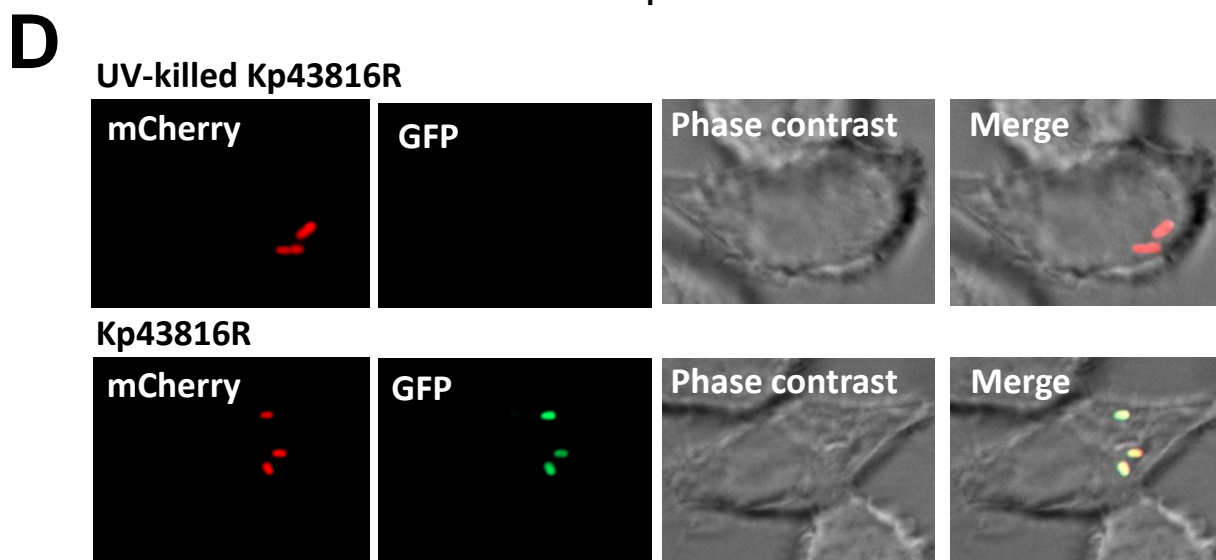
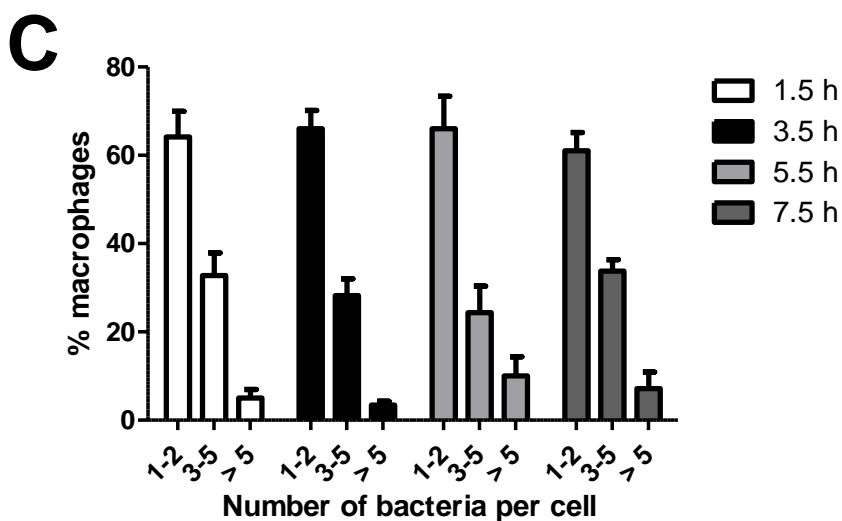
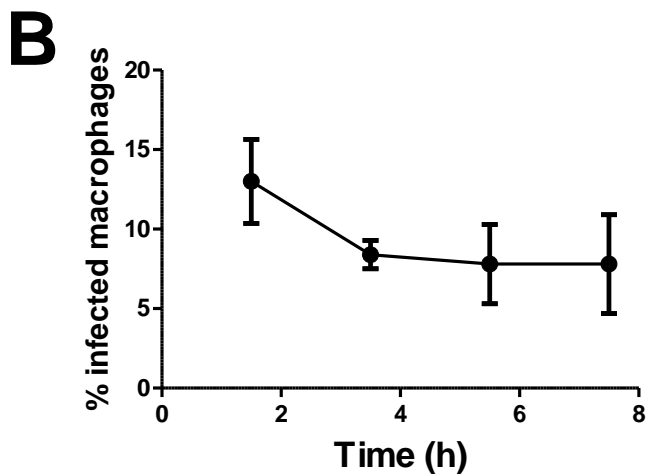
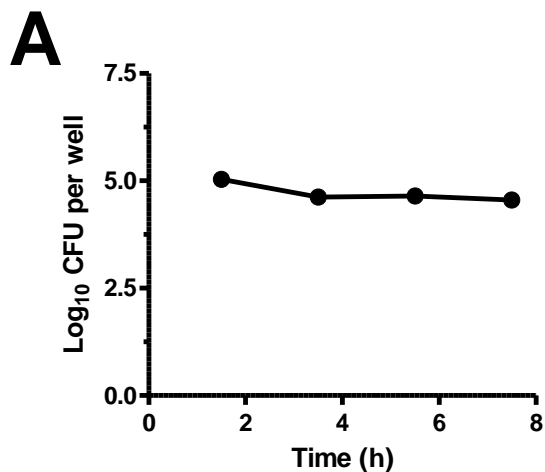
enumeration. Data, shown as CFU/well, are the average of three independent experiments. \*,  $P < 0.05$  (results are significantly different from the results for untreated cells; Mann-Whitney U test). (B) Percentage of Kp43816R colocalization with TR-dextran or cathepsin D in cells mock-treated or treated with the Akt inhibitor AKT X over a time course. Cells were infected, coverslips were fixed and stained at the indicated times. AKT X was added after the time of contact and kept until cells were fixed. Values are given as mean percentage of Kp43816R colocalizing with the marker  $\pm$  SE. At least 300 infected cells belonging to three independent experiments were counted per time point. \*,  $P < 0.05$  (results are significantly different from the results for untreated cells; Mann-Whitney U test). (C) Colocalization of Kp431816R and Lamp1 and EGFP-Rab14 (images were taken 3.5 h post infection). Bacteria were stained using rabbit anti-*Klebsiella* and goat anti-rabbit conjugated to Cascade blue antibodies. Images are representative of triplicate coverslips in three independent experiments. (D) Percentage of Kp43816R colocalization with EGFP-Rab14 over a time course. Cells were infected, coverslips were fixed and stained at the indicated times. Values are given as mean percentage of Kp43816R colocalizing with the marker  $\pm$  SE. At least 300 infected cells belonging to three independent experiments were counted per time point. (E) Quantification of intracellular bacteria in transfected MH-S cells with plasmid pcDNA3 or with Rab14 dominant-negative construct (DN-Rab14) at 3.5 h post infection. Data, shown as CFU/well, are the average of three independent experiments. \*,  $P < 0.05$  (results are significantly different from the results for cells transfected with control plasmid pcDNA3; Mann-Whitney U test). (F) Immunofluorescence showing the lack of colocalization of the KCV and EGFP-Rab14 (images were taken 3.5 h post infection) in AKT X treated cells. Bacteria were stained using rabbit anti-*Klebsiella* and goat anti-rabbit conjugated to Cascade blue antibodies. Images are representative of triplicate coverslips in two independent experiments.

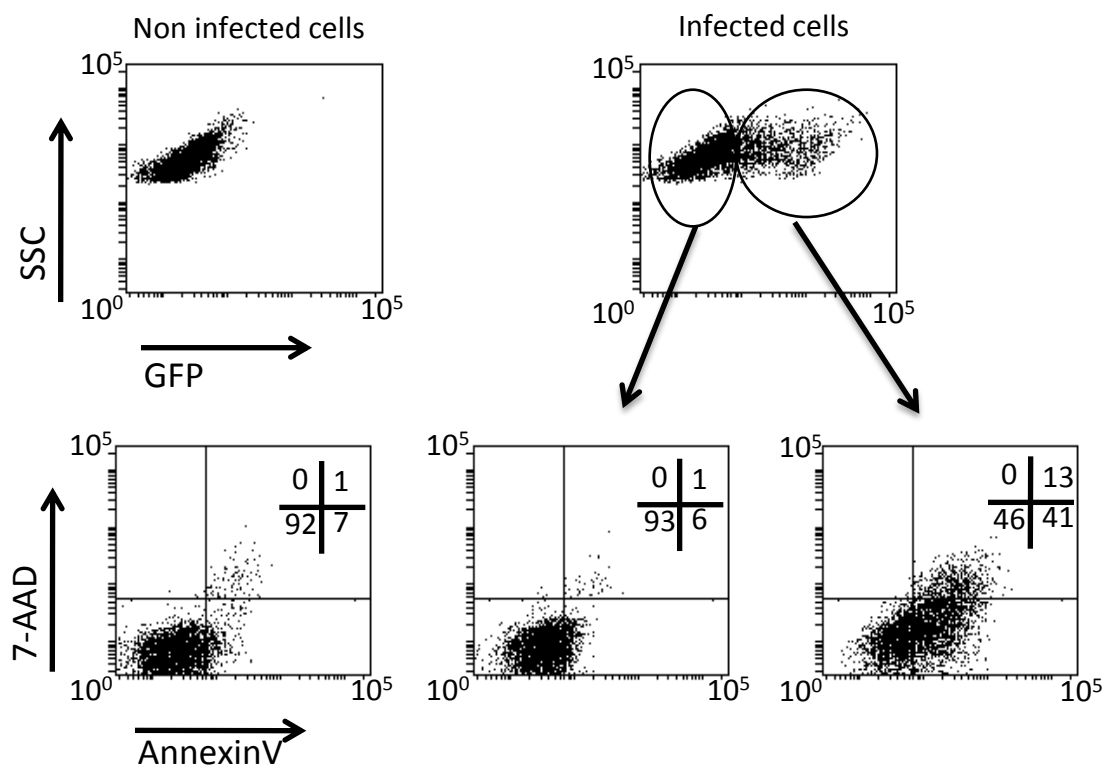
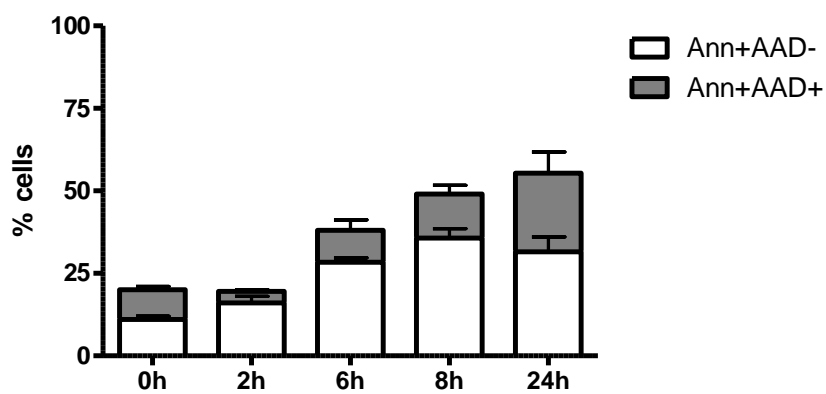
**FIGURE 8. Role of CPS in *K. pneumoniae* intracellular survival.**

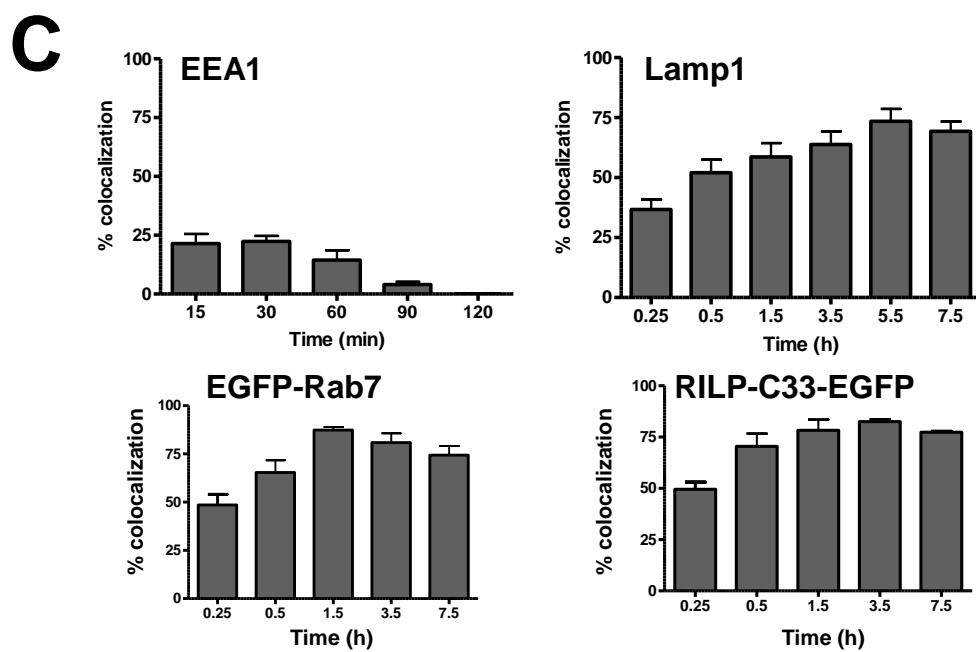
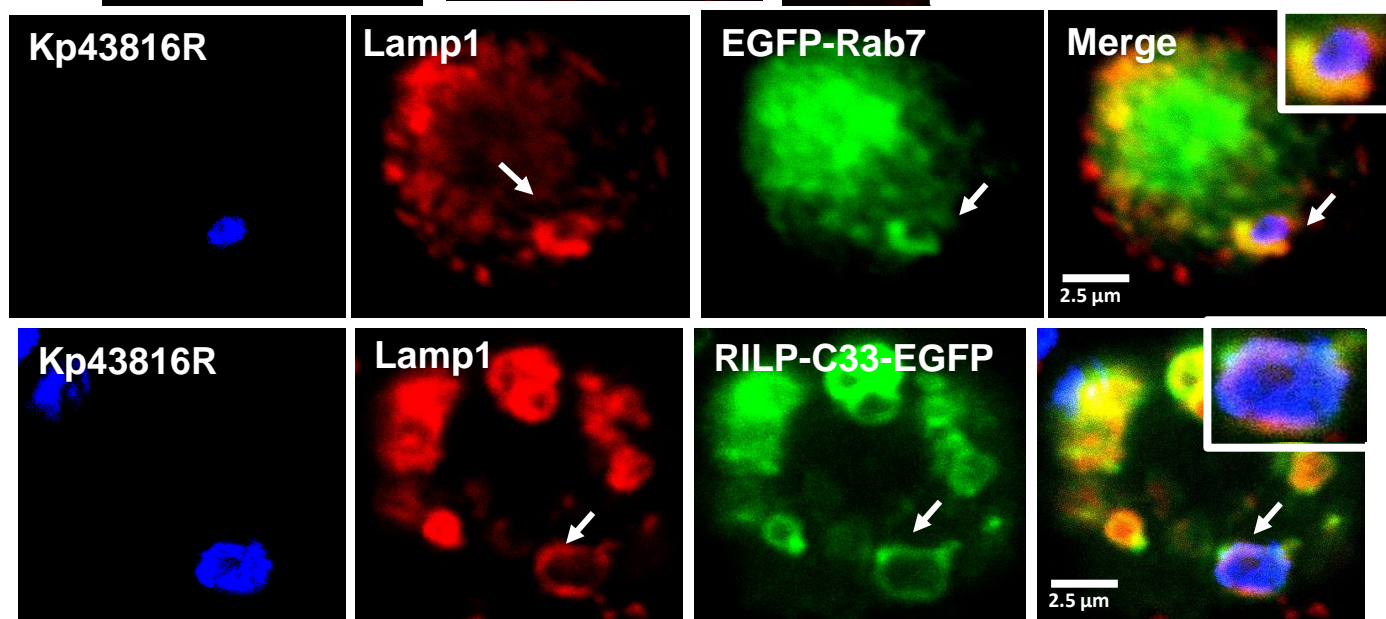
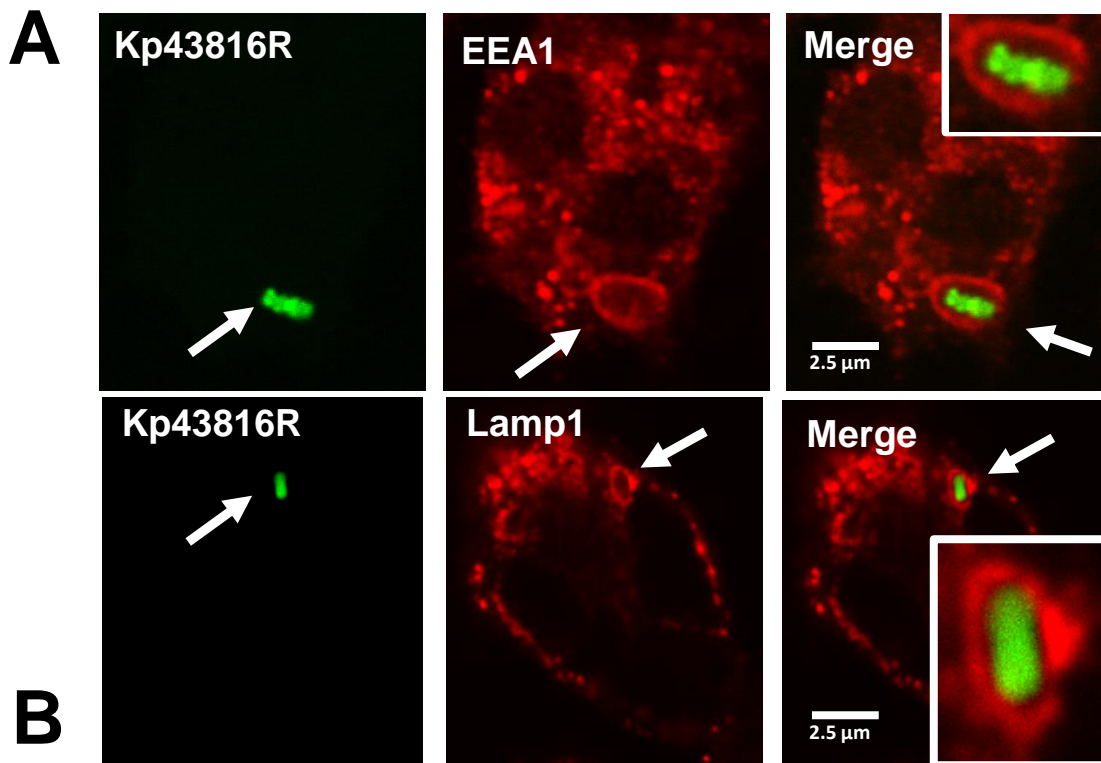
(A) MH-S or mTHP-1 cells were infected with Kp43816R (black symbols) or the capsule mutant (43 $\Delta$ manCKm; white symbols). Intracellular bacteria were quantified by lysis, serial dilution and

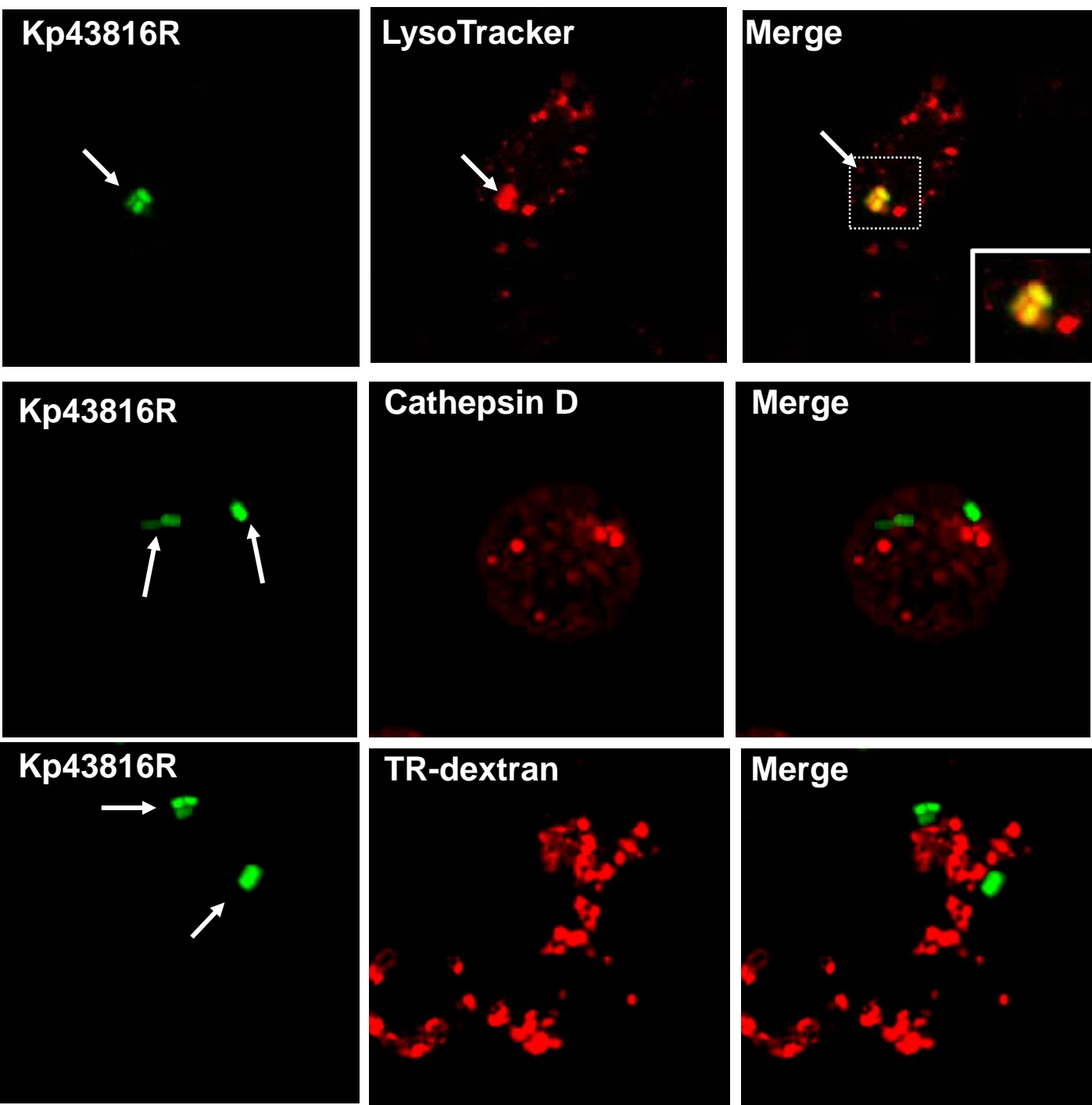
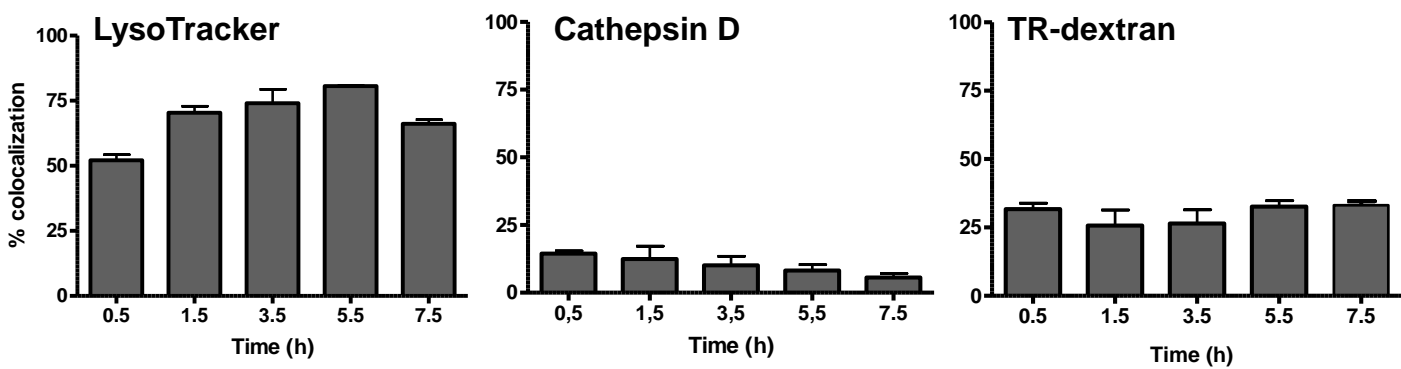
1122 viable counting on LB agar plates. Data, shown as  $\text{Log}_{10}\text{CFU/well}$ , are the average of three  
1123 independent experiments. (B) Opsonization with 1% normal human sera (NHS) increased the  
1124 phagocytosis of the capsule mutant (Kp43816Rdes) by mTHP-1 cells. Data, shown as CFU/well,  
1125 are the average of three independent experiments. \*,  $P < 0.05$  (results are significantly different  
1126 from the results for cells infected with the non-opsonized capsule mutant; Mann-Whitney U  
1127 test); n.s., no significant difference. (C) mTHP-1 cells were infected for 30 min with Kp43816R  
1128 or the capsule mutant ( $43\Delta\text{manCKm}$ ;  $\Delta\text{manCKm}$ ) which were either opsonized or not.  
1129 Intracellular bacteria were quantified by lysis, serial dilution and viable counting on LB agar  
1130 plates. Data, shown as  $\text{Log}_{10}\text{CFU/well}$ , are the average of three independent experiments.  
1131 Significance testing performed by Log Rank test. \*,  $P < 0.05$ . (D) Analysis of *cps::gfp*  
1132 expression over time by flow cytometry. Analysis was performed staining the bacteria using  
1133 rabbit anti-*Klebsiella* and donkey anti-rabbit conjugated to Rhodamine antibodies (red  
1134 histogram). GFP fluorescence (green histogram) was analyzed in the gated Rhodamine labelled  
1135 (antibody stained) population. Grey histogram represents GFP fluorescence for the negative-  
1136 control sample, and the area of the histogram is considered negative for GFP fluorescence.  
1137 Panels show the overlay of the different histograms. Results are representative of three  
1138 independent experiments. (E) Fluorescence levels of Kp43816R containing pPROBE'43Procps.  
1139 Data, shown as relative fluorescence units (RFUs), are the average of three independent  
1140 experiments. \*,  $P < 0.05$  (results are significantly different from the results for cells grown in  
1141 medium buffered to pH 7.5; Mann-Whitney U test). (F) *wzi*, *orf7* and *gnd* mRNA levels assessed  
1142 by RT-qPCR. Data are presented as mean  $\pm$  SD ( $n = 3$ ). \*,  $P < 0.05$  (results are significantly  
1143 different from the results for cells grown in medium buffered to pH 7.5; Mann-Whitney U test).

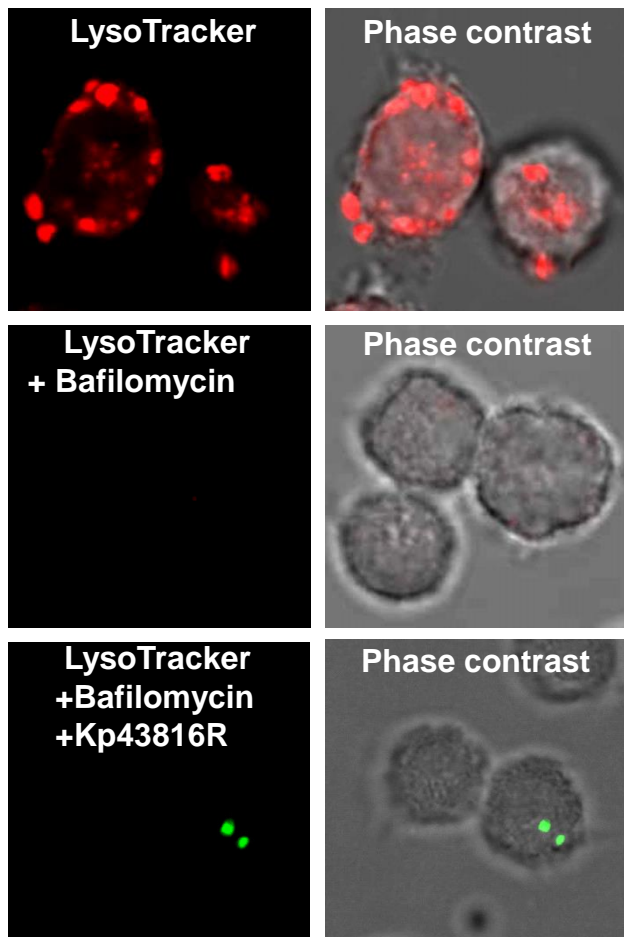
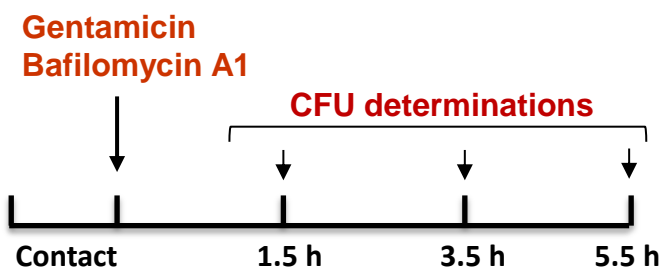
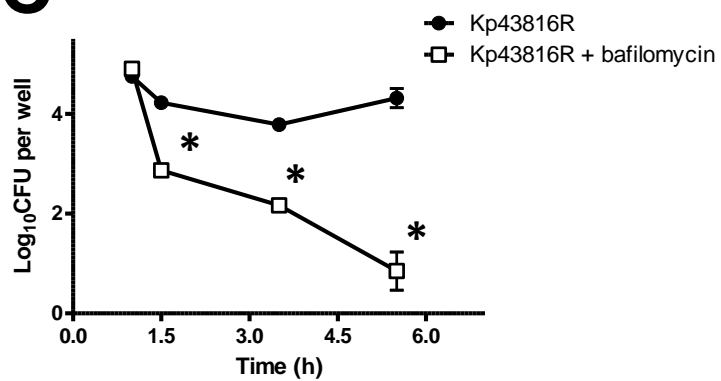
**A****B****C****D**



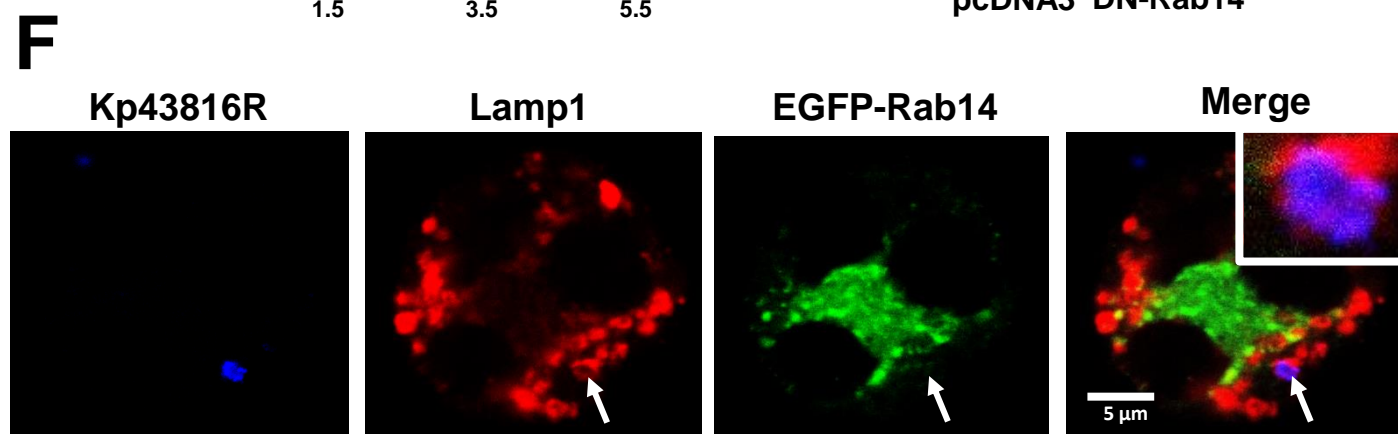
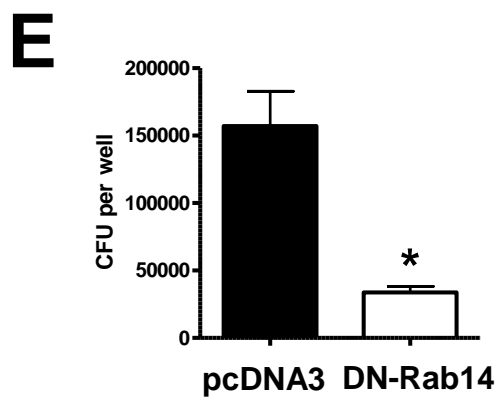
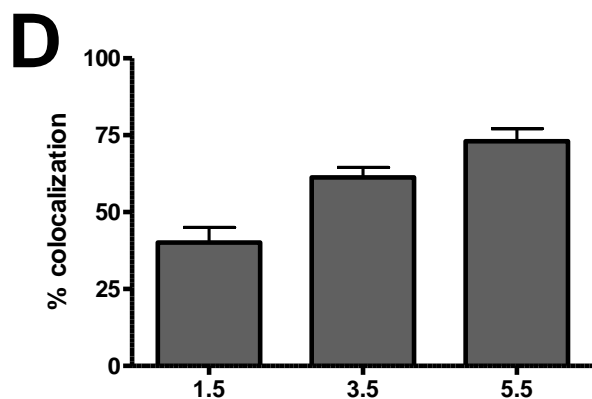
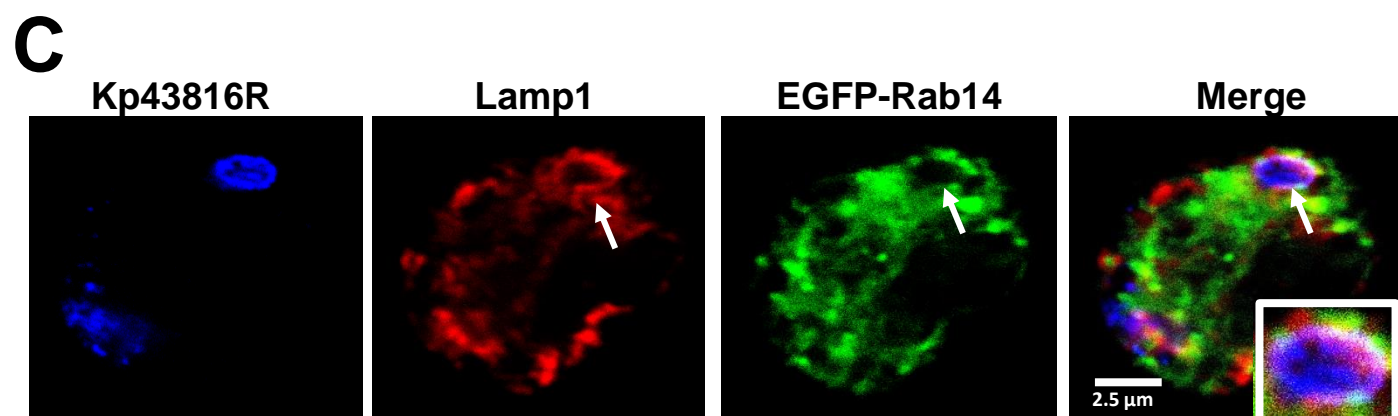
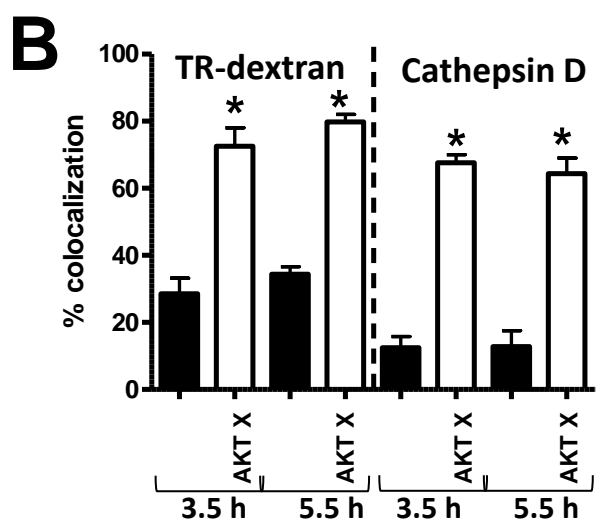
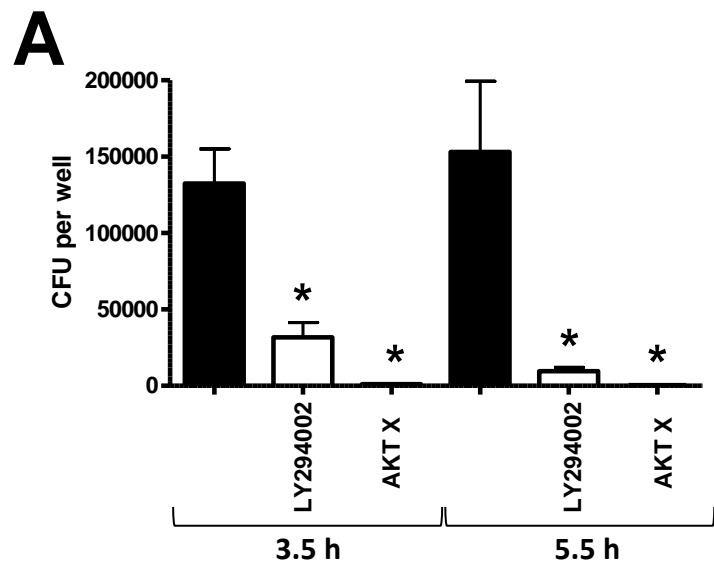
**A****B**

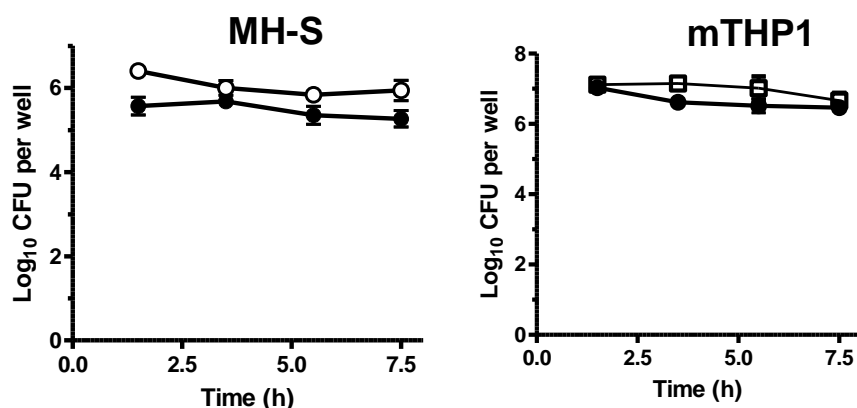
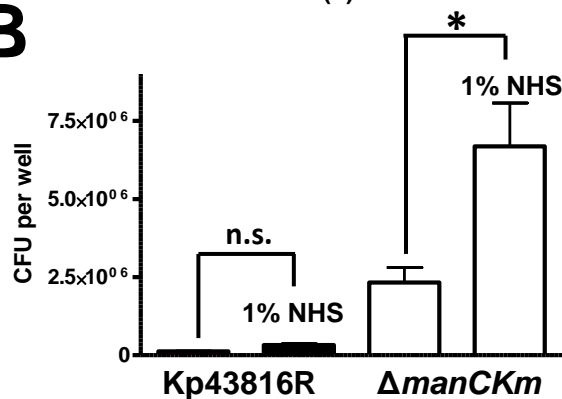
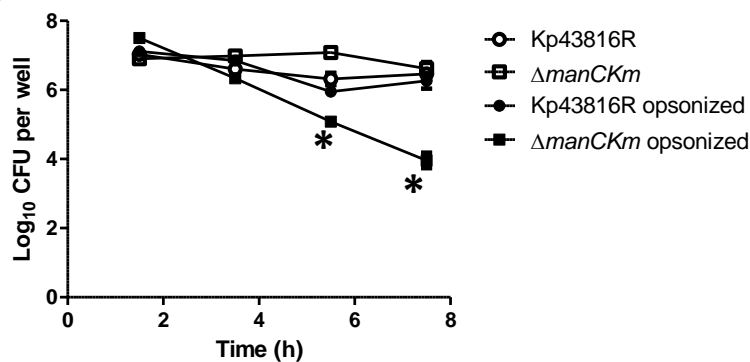
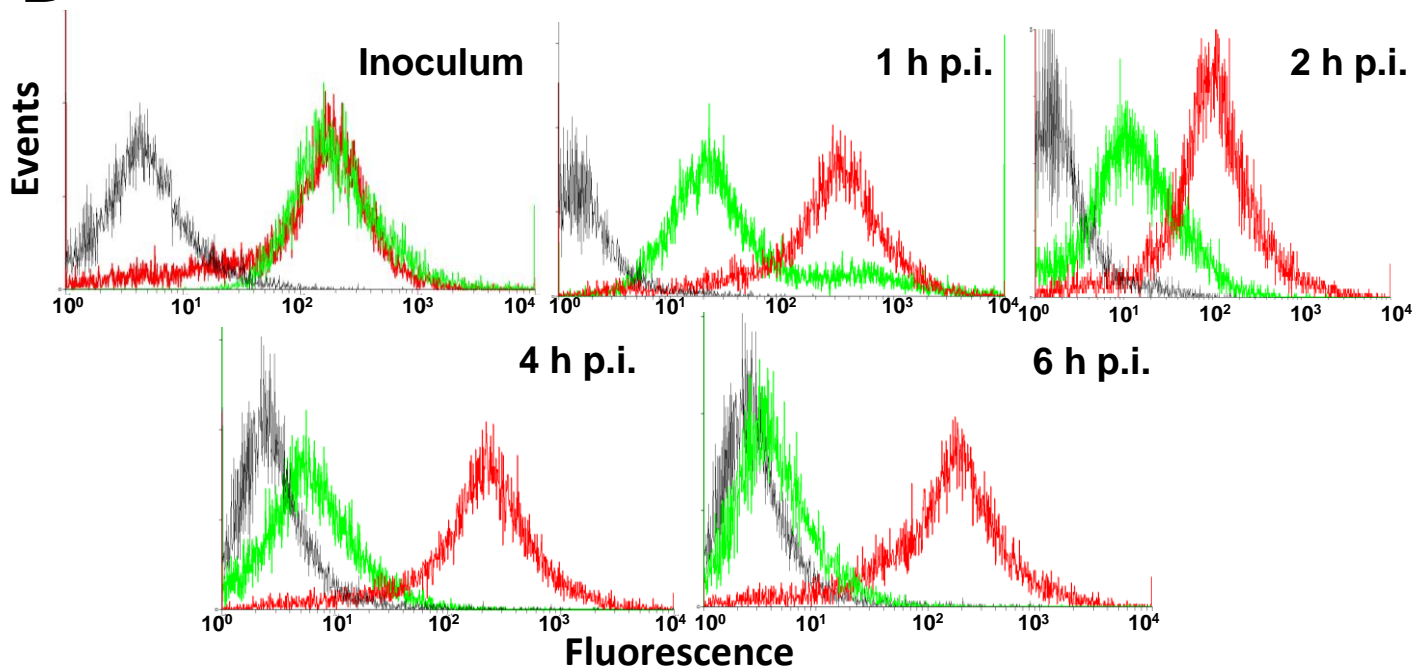
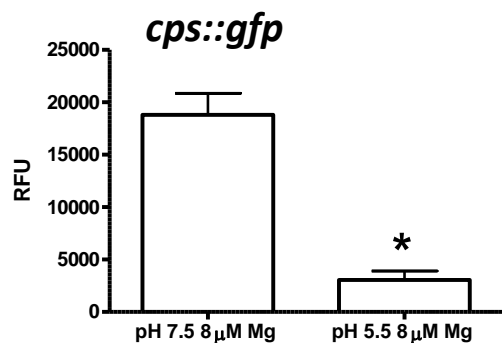


**A****B**

**A****B****C**





**A****B****C****D****E****F**